Title: Molecular dynamics and physical stability of ibuprofen in binary mixtures with an acetylated derivative of maltose

Author: Katarzyna Grzybowska, Andrzej Grzybowski, Justyna Knapik-Kowalczuk, Krzysztof Chmiel, K. Woyna-Orlewicz, J. Szafraniec-Szczęsny, A. Antosik-Rogóż, R. Jachowicz, Katarzyna Kowalska-Szojda, Piotr Lodowski, Marian Paluch

Citation style: Katarzyna Grzybowska, Andrzej Grzybowski, Justyna Knapik-Kowalczuk, Krzysztof Chmiel, Woyna-Orlewicz K., Szafraniec-Szczęsny J., Antosik-Rogóż A., Jachowicz R., Katarzyna Kowalska-Szojda, Piotr Lodowski, Marian Paluch. (2020). Molecular dynamics and physical stability of ibuprofen in binary mixtures with an acetylated derivative of maltose. "Molecular Pharmaceutics" iss. 8, (2020), s. 3087-3105. DOI: 10.1021/acs.molpharmaceut.0c00517

molecular pharmaceutics

pubs.acs.org/molecularpharmaceutics

Article

Molecular Dynamics and Physical Stability of Ibuprofen in Binary Mixtures with an Acetylated Derivative of Maltose

Katarzyna Grzybowska,* Andrzej Grzybowski, Justyna Knapik-Kowalczuk, Krzysztof Chmiel, Krzysztof Woyna-Orlewicz, Joanna Szafraniec-Szczęsny, Agata Antosik-Rogóż, Renata Jachowicz, Katarzyna Kowalska-Szojda, Piotr Lodowski, and Marian Paluch

Cite This: *Mol. Pharmaceutics* 2020, 17, 3087−3105

Read Online

ACCESS | Metrics & More | Article Recommendations

ABSTRACT: In this paper, we explore the strategy increasingly used to improve the bioavailability of poorly water-soluble crystalline drugs by formulating their amorphous solid dispersions. We focus on the potential application of a low molecular weight excipient octaacetyl-maltose (acMAL) to prepare physically stable amorphous solid dispersions with ibuprofen (IBU) aimed at enhancing water solubility of the drug compared to that of its crystalline counterpart. We thoroughly investigate global and local molecular dynamics, thermal properties, and physical stability of the IBU+acMAL binary systems by using broadband dielectric spectroscopy and differential scanning calorimetry as well as test their water solubility and dissolution rate. The obtained results are extensively discussed by analyzing several factors considered to affect the physical stability of amorphous systems, including those related to the global mobility, such as plasticization/antiplasticization effects, the activation energy, fragility parameter, and the number of dynamically correlated molecules as well as specific intermolecular interactions like hydrogen bonds, supporting the latter by density functional theory calculations. The observations made for the IBU+acMAL binary systems and drawn recommendations give a better insight into our understanding of molecular mechanisms governing the physical stability of amorphous solid dispersions.

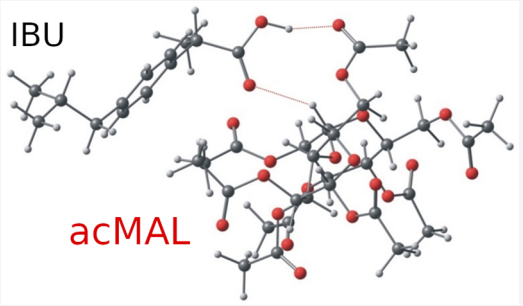

KEYWORDS: *ibuprofen, amorphous drug, amorphous solid dispersion, molecular dynamics, glass transition, crystallization, devitrification, physical stability*

INTRODUCTION

Many pharmaceutical compounds in the crystalline state are thermodynamically stable materials; their properties are well-defined, but they often have a low water solubility, leading to low dissolution rate and bioavailability. One of many popular drugs, the crystalline form of which is practically insoluble in water, is ibuprofen (IBU). Ibuprofen is a nonsteroidal anti-inflammatory drug commonly used to reduce fever, pain, and stiffness. According to the Biopharmaceutical Classification System (BCS), IBU has been classified as a class II drug, which means that it has a poor solubility despite the good permeability.[1] Thus, the low oral bioavailability of IBU is due to its solubility and dissolution rate limitations.[2] Such properties for a painkiller are unfavorable because the fastest possible dissolution rate of an analgesic drug associated with its rapid onset of action is essential in the case of pain situations (particularly in rheumatoid, osteoarthritis, or dental pain). Considering the widespread use of IBU, the improvement of water solubility and the dissolution rate of the drug is a rational and ambitious challenge.

Transformation of the crystalline form of a drug into a less ordered amorphous structure is one of the key formulation technologies in the pharmaceutical industry because amorphous solids are usually characterized by higher solubility and higher dissolution rate than corresponding crystals.[3−12] Despite the obvious useful properties of amorphous drugs, so far, only a few oral amorphous formulations have been available on the market because of various problems. One of the most unfavorable aspects of the amorphous formulations is their poor physical stability due to higher internal energy and specific volume of the amorphous state relative to the crystalline state.[13] The molecular mobility is generally considered as a key attribute that determines the physical stability of the amorphous drugs.[14−16] A relatively high molecular mobility in glassy systems can lead to faster phase separation, drug nucleation, and crystal growth. Consequently,

Received: May 11, 2020
Revised: June 24, 2020
Accepted: June 25, 2020
Published: June 25, 2020

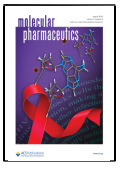

https://dx.doi.org/10.1021/acs.molpharmaceut.0c00517
Mol. Pharmaceutics 2020, 17, 3087−3105

amorphous drugs may spontaneously convert back to crystalline forms during production, storage, and use of the product, losing the desired properties associated with the disordered structure of the glasses.

In recent years, many efforts have been put into finding effective methods for improving the physical stability of amorphous pharmaceuticals. A promising way to reduce the tendency of amorphous drugs to crystallize and enhance their water solubility by formulating it as amorphous solid dispersions with certain excipients, including polymers (polymeric amorphous solid dispersion)[17] and low molecular weight compounds such as saccharides,[18] amino sugars,[19] acetated saccharides,[10,20−22] urea,[23] amino acids,[24] organic acids,[25] or other drugs (coamorphous solid dispersions).[26,27] The tendency of the drug to crystallize may be reduced in amorphous solid dispersions mainly by interplaying two factors:[28−30] (i) specific intermolecular interactions between molecules of drug and excipient or/and (ii) slowing down the global molecular mobility in the mixture associated with the structural relaxation or/and local molecular motion linked to secondary relaxations.

Decreasing the global molecular mobility may be achieved by mixing an amorphous drug that has a low glass transition temperature T_g with a high T_g compound (usually with polymers). In such a binary mixture, a high T_g excipient is an antiplasticizer of a drug; that is, it causes an increase in T_g of the binary mixture (drug−excipient) compared with T_g of pure API. The increase in T_g of the binary composition is associated with a decrease in the mobility of whole molecules of a pharmaceutical and, consequently, with a reduction in the tendency to the drug crystallization in the glassy solution. However, the antiplasticization is not always sufficient to completely suppress the recrystallization,[31,20] and for some drugs, crystallization can be completely inhibited without any antiplasticizing effect.[20] The mechanism of crystallization inhibition in such cases is mainly related to the specific intermolecular interactions between drug and excipient, such as hydrogen bonds or ionic interactions. Molecules of an excipient, which are able to specifically interact with the drug molecules, prevent the recrystallization process of the drug.[10,31−33,22]

In this context, the amorphous solid dispersions of drugs with the use of an acetylated derivative of sugars as crystallization inhibitors are very interesting. Grzybowska and co-workers[10] were the first to use small molecular weight octaacetylmaltose (acMAL) to effectively inhibit celecoxib (CEL) crystallization in the binary glassy solution (CEL +acMAL). They found that even a small content (10%) of acMAL in the solution completely counteracts the recrystallization of the glassy state. In this system, the antiplasticization effect does not play any role in this way of physical stabilization of amorphous CEL because the values of T_g of both compounds (drug and excipient) are the same (T_g = 331 K). Indeed, no increase in T_g of the amorphous binary systems was found due to the addition of acMAL to the drug, and even the values of T_g for the CEL-acMAL glassy solution were slightly lower than that for pure celecoxib. Whereas, the stabilizing effect of acMAL on the CEL has been correlated with the slowing down of local molecular movements in the binary glassy solution (CEL+acMAL) reflected in the dielectric secondary (β- and γ-) relaxations. It has been established that significant suppression of local mobility of glassy CEL in the acMAL matrix reflected in both the intermolecular (β-process) and intramolecular (γ-process) is a result of strong hydrogen bonds formed between CEL and the —C═O group of acMAL. Moreover, the application of acMAL significantly enhanced not only the physical stability but also the water solubility of CEL in the binary glassy solutions (CEL +acMAL). The water solubility of pure amorphous CEL was only 1.5 times better than its crystalline counterpart, whereas the water solubility of the amorphous CEL systems containing 10 and 30 wt % of acMAL was, respectively, 6 and 12 times greater than that for the crystalline drug. The pioneering application of acMAL to effectively stabilize amorphous CEL and also to improve its water solubility has inspired further successful attempts[21,22] at exploiting acetylated saccharides as crystallization inhibitors of other amorphous pharmaceuticals. Kaminska et al. have shown that acMAL might be very effective in stabilizing the amorphous form of indomethacin (IMC).[22] The authors found that strong interactions between the IMC and acMAL by forming hydrogen bonds between molecules of both compounds led to the improvement in the physical stability of amorphous API even at temperatures higher than T_g of the binary systems. The water solubility of amorphous IMC was also enhanced in solid dispersions with acMAL. Another study also proved the stabilizing effect of different acetylated saccharides, such as acetylated maltose, sucrose, glucose, and galactose on nifedipine (NIF) in the binary glassy solutions.[21] It has been found that hydrogen bonds between NIF and acetated disaccharides are stronger than H-bonds interactions between NIF and acetated monosaccharides. It has been correlated with a higher crystallization barrier for crystallization binary solid dispersion of NIF with acetated disaccharides and, consequently, with better stabilization of the drug in such binary systems both above and below the glass transition temperature. Acetylated sugars like maltose, sucrose, and glucose have also been used to increase the chemical stability of furosemide,[34] which easily degraded as a neat drug upon melting or cryogenic grinding. Theoretical computations have indicated that H-bonds play an important role in the destabilization mechanism of furosemide upon milling. Kaminska et al. shown that acylated saccharides like maltose, sucrose, and glucose inhibit the chemical decomposition of furosemide during the cryomilling of the binary mixtures. This effect was attributed to the reduction in H-bonds formation between the API and the modified carbohydrates. Moreover, furosemide cryomilled with acylated glucose, acylated maltose, and acylated sucrose is much more soluble with respect to the crystalline form of this active pharmaceutical ingredient (API).[34]

In this work, we investigate the effects of adding low molecular weight octaacetyl-maltose (acMAL) on the molecular dynamics, thermal properties, and the physical stability of ibuprofen (IBU) in the binary mixtures (IBU+acMAL). Although acMAL has a low molecular weight, its glass transition temperature T_g is much higher than that for IBU. Thus, one can suppose that the excipient will be a good antiplasticizer of IBU. By using the broadband dielectric spectroscopy and differential scanning calorimetry, we check the role of the antiplasticization effect of acMAL on the drug as well as other molecular and thermodynamic factors on the enhancement of the physical stability of IBU in binary mixtures (IBU+acMAL). Exploiting theoretical calculations within the framework of the density functional theory (DFT), we study specific interactions between molecules of both compounds in the binary mixtures (IBU-acMAL) and their potential role in

https://dx.doi.org/10.1021/acs.molpharmaceut.0c00517
Mol. Pharmaceutics 2020, 17, 3087−3105

Chart 1. Chemical Structures of Investigated Compounds

API	Excipient
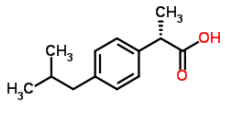 **Ibuprofen (IBU)** (M_{w_IBU} = 206.28g/mol)	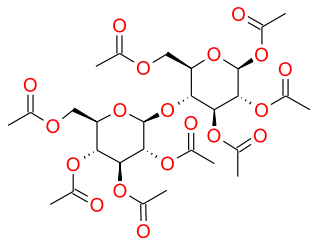 **Octa-acetyl-maltose (acMAL)** M_{w_acMAL} = 678.59g/mol

crystallization inhibition of IBU by acMAL. Finally, we examine whether the excipient acMAL in the binary mixtures (IBU-acMAL) improves the water solubility of the drug. Such studies are essential for the evaluation of acMAL as a potential excipient for manufacturing solid dosage forms of IBU of improved bioavailability.

EXPERIMENTAL METHODS

Materials. The crystalline form of ibuprofen (IBU) of the molecular mass of 206.28 g/mol and 98% purity was supplied from Sigma-Aldrich. β-D-Maltose octaacetate (acMAL) of a molecular mass of 678.59 g/mol was supplied from Iris Biotech GMBH (Germany) in the crystalline form. Chemical structures of the examined materials are presented in Chart 1.

Method of Preparation of Amorphous Solid Dispersions IBU with acMAL. The amorphous binary systems IBU+acMAL with different amounts of excipient (acMAL) were prepared by a quench-cooling of the molten phase of the binary mixtures. Before preparing the binary mixtures of IBU +acMAL with a small content of acMAL ($\lesssim$30 wt % of acMAL), the pure crystalline acMAL was vitrified and powdered at room temperature, whereas the pure crystalline ibuprofen was heated slightly above its melting point (up to 95 °C) on the heating plate. Next, a sufficient amount of powdered amorphous acMAL was added to the molten ibuprofen and intensively mixed until a homogeneous binary mixture was obtained. For larger content of acMAL ($\gtrsim$30 wt %), the mixture became supersaturated and crystallized during the maltose dissolving procedure in liquid ibuprofen. To obtain the binary mixtures (IBU+acMAL) with a larger content of acMAL, the drug in the crystalline form had to be dissolved in the molten phase of acMAL.

Broadband Dielectric Spectroscopy Measurements (BDS). Isobaric measurements of the dielectric permittivity $\varepsilon^*(\omega) = \varepsilon'(\omega) - i''(\omega)$ were performed using the Novocontrol Alpha dielectric spectrometer over a frequency range (10^{-2}–10^6 Hz) and a temperature range (120–320 K) at ambient pressure. Nonisothermal and isothermal dielectric measurements of IBU+acMAL mixtures were performed in a parallel-plate cell immediately after preparing the amorphous sample. The sample temperatures were controlled by the Quatro System using a nitrogen gas cryostat. The temperature stability was better than 0.1 K. To confirm the repeatability of measurements, each measurement was repeated three times for newly prepared samples.

Differential Scanning Calorimetry (DSC). Calorimetric measurements of the investigated binary mixtures were carried out by the Mettler-Toledo DSC apparatus equipped with a liquid nitrogen cooling accessory and an HSS8 ceramic sensor (heat flux sensor with 120 thermocouples). Temperature and enthalpy calibrations were performed by using indium and zinc standards. Each measurement at the given heating rate was repeated 3 times. For each experiment, a new amorphous sample was prepared.

To obtain the accurate temperature dependences of heat capacity $C_p(T)$ for examined mixtures and temperature dependences of calorimetric structural relaxation times for binary mixtures of IBU+acMAL, a stochastic temperature-modulated differential scanning calorimetry (TMDSC) technique implemented by Mettler-Toledo TOPEM has been exploited. The samples were heated at a rate of 0.5 K/min. In the experiment, the temperature amplitude of the pulses of 0.5 K was selected. To achieve a higher accuracy of the heat capacity, we adjusted our evaluations using a sapphire reference curve. The glass transition temperature T_g was determined as the temperature of the half step height of the temperature dependences of the quasi-static heat capacity $C_p(T)$.

Computational (DFT). Theoretical studies were performed within the framework of the density functional theory. DFT calculations have been done using the B3LYP[35−37] functional and def2-TZVP basis set.[38] The environment of molecular systems was taken into account by applying the PCM continuum solvation model[39,40] with dielectric constant ε = 2.5. The molecular structures of the IBU and acMAL monomers, IBU homodimer, and IBU+acMAL complex were fully optimized without any constraints at the DFT level of theory. Grimme's D3 dispersion correction for a density functional[41] was applied in order to include intramolecular and intermolecular dispersion interactions. The association energy for IBU homodimer and IBU-acMAL heterodimer has been estimated using the supermolecular approach. For IBU, to obtain the potential energy curve (PEC) and dipole moments as a function of the selected rotation coordinate, the single-point calculations were performed for four selected torsion angles (see Figure 12) in a range from 0 to 360 with a step size of 10 degrees. In each point, corresponding torsion coordinates in the molecular structure were frozen and excluded from optimization, and at once, the remaining geometrical parameters were relaxed. All calculations were performed using Gaussian 09 quantum-chemical software.[42]

Solubility Test. The solubility studies were performed in purified water for binary mixtures of IBU with the large content of acMAL (IBU+83 wt % acMAL, IBU+86 wt %

https://dx.doi.org/10.1021/acs.molpharmaceut.0c00517
Mol. Pharmaceutics 2020, 17, 3087−3105

acMAL, and IBU+87.5 wt % acMAL). Each study was performed in 50 mL Erlenmeyer flasks. An excess of drug or binary system was dispersed in 25 mL of the solvent. The suspension was shaken at room temperature using the KS 130 Basic shaker (IKA, Germany) for at least 24 h to achieve the equilibrium solubility. Samples were centrifuged at 3600 rpm for 30 min in the MPW 221 apparatus (MPW, Poland) and filtered through a 0.2 μm membrane filter. The samples were assayed at 221 nm with the UV−vis spectrophotometer V-500 (Shimazu UV1800, Japan). The reported data represents the averages from three measurements.

Dissolution Studies. The IBU release profile was tested in the Hanson Research SR8PLUS dissolution station combined with Dissoette II Autosampler and spectrophotometer UV/vis Jasco V530 for binary mixtures of IBU with the large content of acMAL (IBU+83 wt % acMAL, IBU+86 wt % acMAL, and IBU+87.5 wt % acMAL). The studies were performed in Ph.Eur. app.2 at 50 rpm. The tested samples containing 50 mg of IB were poured into vessels filled with 900 mL of purified water preheated up to 37 ± 0.5 °C. The IBU concentration was determined spectrophotometrically at 221 nm.

RESULTS AND DISCUSSION

To determine the thermal properties of pure compounds (IBU and acMAL) used to prepare binary mixtures, the standard calorimetric measurements by means of differential scanning calorimetry (DSC) have been performed (see Figure 1). IBU

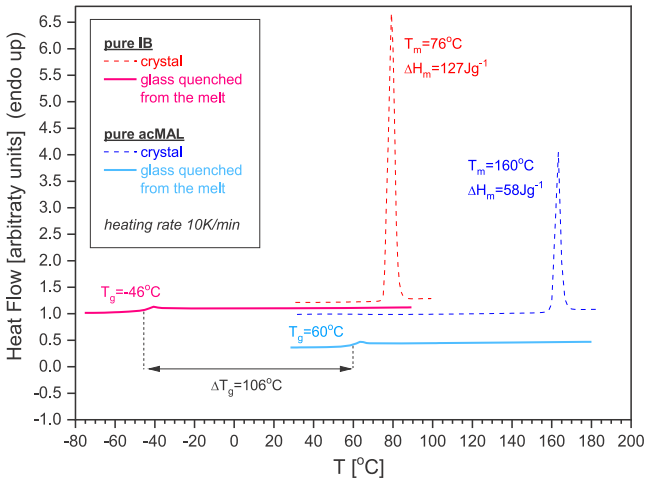

Figure 1. DSC thermograms of the pure IBU and acMAL obtained during heating (10 K/min), their crystalline and amorphous forms. The first run was performed for crystalline samples (dashed lines), whereas the second one for amorphous samples (solid lines) was obtained by cooling the fully melted crystals below the glass transition temperatures T_g (vitrification).

has a low melting temperature, T_m = 76 °C, and a low glass transition temperature, T_g = −46 °C. Due to that, IBU after vitrification is not an amorphous solid at ambient temperatures, but it is a viscous, supercooled liquid. Therefore, under normal conditions, IBU cannot be prepared as an amorphous oral solid dosage form (tablets) without using appropriate excipients. Octaacetylmaltose (acMAL) is characterized by a much higher T_g (=60 °C) than that for IBU. Mixing of two compounds characterized by different glass transition temperatures typically results in a higher T_g of the binary mixture (drug−excipient) compared to T_g of pure API if the low T_g compound is the API. Thus, we may suppose that acMAL will be a good antiplasticizer of IBU and significantly increase T_g of the binary composition (IB+acMAL) from that of the pure drug to obtain the amorphous solid dispersion characterized by the high physical stability in ambient conditions.

Molecular Dynamics of Binary Mixtures (IBU+acMAL). *Relaxation Processes at $T > T_g$.* The broadband dielectric spectroscopy (BDS) measurements of pure compounds (IBU and acMAL), as well as their binary mixtures with different content (5, 10, 20, and 30 wt %) of acMAL, have been performed to check how a gradual adding acMAL to IBU affects the molecular mobility of IBU and, consequently, its stability in the wide temperature range. Representative dielectric loss spectra for investigated systems measured at different temperatures during heating of the samples from the glassy to the liquid state are presented in Figure 2.

It is clearly seen that the dielectric spectra for the supercooled liquid state of the examined mixtures (IBU +acMAL) are more complex in comparison with spectra of most glass-forming liquids, for which usually only a single relaxation process (i.e., structural α-relaxation) with a large magnitude is observed at $T > T_g$. In the case of IBU+acMAL mixtures, above their T_g, we can distinguish two well-resolved relaxation processes with relatively large amplitudes. Based on TMDSC measurements (the results of which will be shown later), we identify the faster dielectric process as a structural α-relaxation of the mixtures, associated with the glass transition of the investigated binary systems. The peculiar dielectric process, slower than the α-relaxation, has been called by us as an s-process. We noticed that the amplitude of the s-process strongly depends on the content of acMAL in the mixture in comparison with α-relaxation. This finding is clearly seen in Figure 3, in which the representative dielectric spectra are collected for pure IBU as well as for its binary mixtures with different content of acMAL measured at the same temperature (T = 259 K > T_g). If the content of acMAL in the mixture is low, the amplitude of the s-process is much smaller than that for the α-process. The gradual addition of acMAL to IBU results in an increase in dielectric strength $\Delta\varepsilon_s$ of s-process. If the amount of acMAL in the mixture reaches ∼20 wt %, the amplitudes of both processes ($\Delta\varepsilon_\alpha$ and $\Delta\varepsilon_s$) become comparable (see a representative example in the inset to Figure 3). The spectacular increase in the dielectric strength $\Delta\varepsilon_s$ of the s-relaxation process with increasing acMAL content in the mixture suggests that the s-relaxation reflects mainly the acMAL dynamics in the (IBU+acMAL) mixture.

Two relaxation processes detected in dielectric spectra above T_g may suggest inhomogeneity of the binary systems and microphase separation.[43,22] Therefore, it is necessary to verify whether the investigated binary mixtures IBU+acMAL are homogeneous, and the s-process observed above T_g is not a result of some phase separations of IBU and acMAL. Exploring this issue, we have not observed any visual signs of phase separation in the examined mixtures. Moreover, we checked whether the dielectric spectrum of the freshly prepared sample of the binary mixture IBU+10 wt % acMAL changes with the time of the sample storage at a given temperature. As can be seen in Figure 4, the dielectric spectrum of the mixture with 10 wt % of acMAL does not change even after 9 h of the sample storage at T = 247 K. This result shows that there are no changes in both the α- and s-relaxations, and consequently, there is no phase separation in the binary mixtures IBU +acMAL at least during the time-dependent dielectric

https://dx.doi.org/10.1021/acs.molpharmaceut.0c00517
Mol. Pharmaceutics 2020, 17, 3087−3105

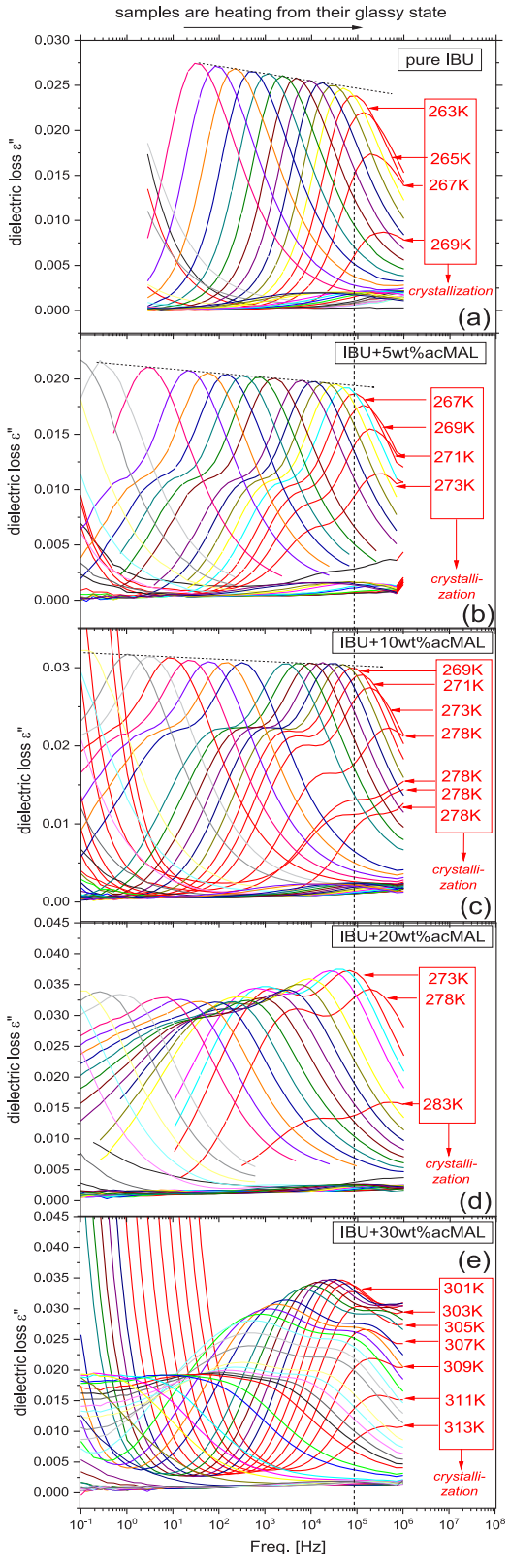

Figure 2. Dielectric loss spectra for pure IBU (a) and for its binary mixtures with 5 wt % (b), 10 wt % (c), 20 wt % (d), and 30 wt % (e) of acMAL at several temperatures.

experiment. This conclusion is also supported by other experimental observations: (i) dielectric measurements are repeatable for each newly prepared sample of a binary mixture; (ii) in DSC thermograms obtained for each investigated binary

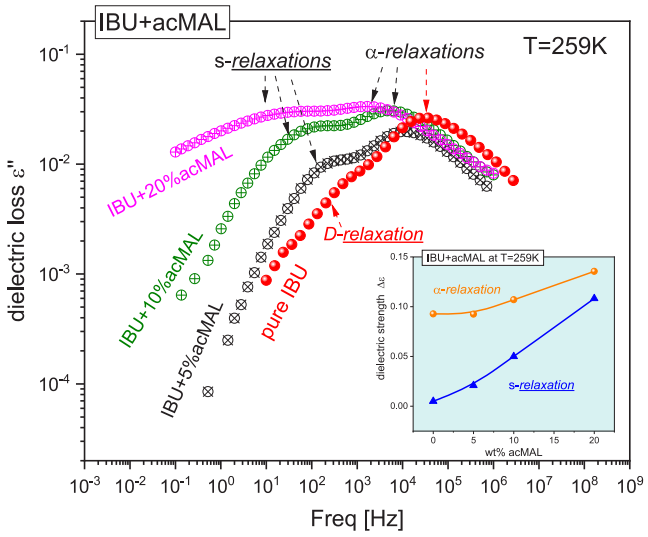

Figure 3. Dielectric loss spectra for pure IBU and for its binary mixtures with 5, 10, and 20 wt % of acMAL obtained at the same temperature, T = 259 K. The inset shows the dependence of the dielectric strength of the α- and s-processes vs content of acMAL in the binary mixtures (IBU+acMAL) at T = 259 K.

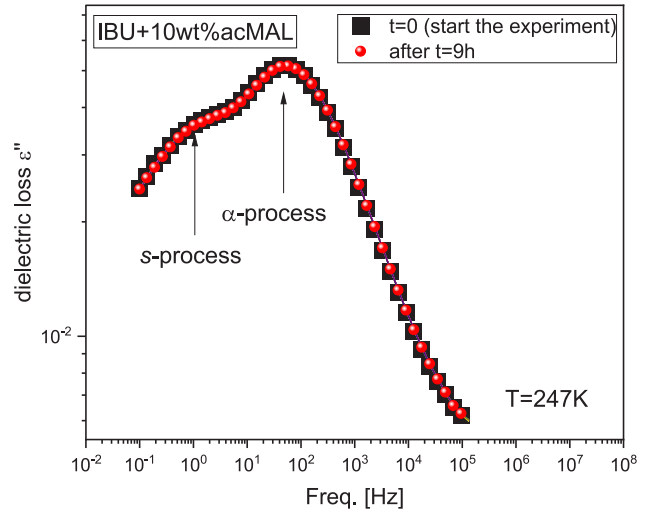

Figure 4. Dielectric loss spectra for a mixture of IBU+10 wt % acMAL obtained immediately after sample preparation at T = 247 K (black points) and after 9 h of its storage at the same temperature (red points).

mixtures, we observed only a single glass transition (T_g sof IBU and acMAL differ significantly, ΔT_g = 106 K, and therefore, in the case of phase separation one may observe two well-distinguished glass transitions for each compound in DSC thermograms). It is worth noting that a previous study of water mixtures with some propylene glycol oligomers leads to the conclusion that the occurrence of two relaxation peaks in dielectric spectra above T_g of the binary systems does not always have to mean the system inhomogeneity and micro-phase separation. For those binary systems (i.e., tripropylene glycol+H_2O and PPG 400+H_2O), the components of which are characterized by excellent miscibility, also two well-distinguished relaxation peaks with large amplitudes were observed: the slower one was the α-relaxation associated with the glass transition of the binary system, whereas the faster one reflected the molecular dynamics of water molecules in the

https://dx.doi.org/10.1021/acs.molpharmaceut.0c00517
Mol. Pharmaceutics 2020, 17, 3087−3105

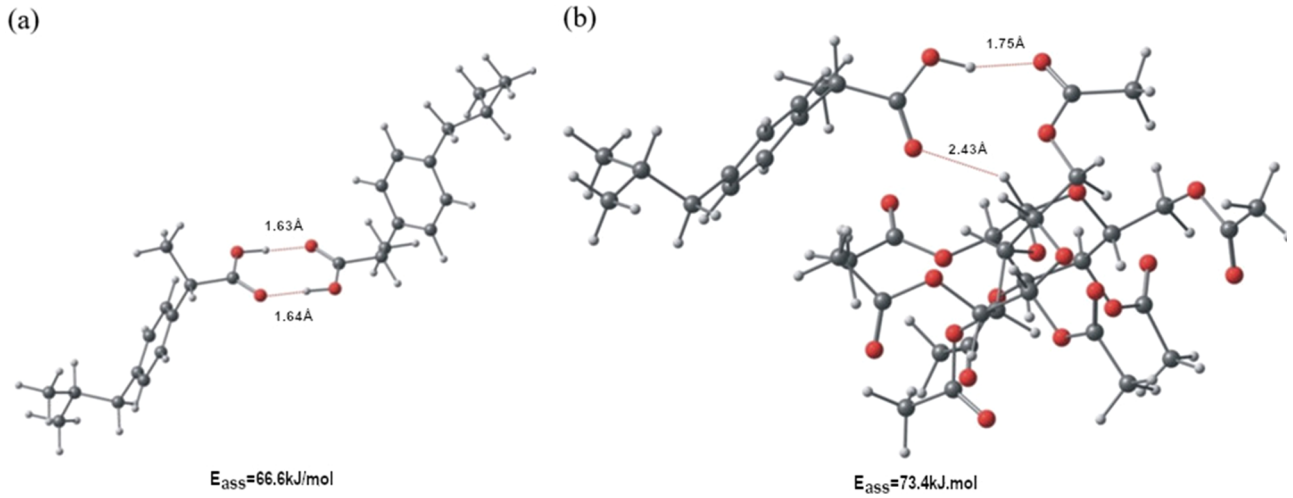

Figure 5. Molecular structure of the ibuprofen homodimer (a) and ibuprofen-acMal complex (b). Geometry of structures optimized at the DFT/B3LYP/Def2-TZVP level of theory.

mixtures.[44,45] Another interesting example of the relaxation spectra involving two segmental processes of comparable amplitudes have been recently reported by Vagelis et al. for perfectly miscible binary blends of polystyrene with oligostyrene.[46]

It is very interesting that the broad and symmetric s-process in the binary mixtures (IBU+acMAL) occurs in a similar frequency range in which the Debye relaxation (D-process) is observed in pure IBU (see Figure 2). The molecular origin of the D-process observed in pure IBU has already been widely discussed.[47−51] Pure IBU has a big tendency to form H-bonded aggregates such as dimers and trimers (linear and cyclic), and the molecular origin of this process has been related to H-bonds dynamics. Correia and Affuard showed that the D-process in pure IBU is dominated by the *cis-* to *trans-*transformation of the carboxyl group (O═C—O—H) in IBU coupled to H-bonds dynamics.[50] Recently, Adrjanowicz and co-workers have established that the D-process can be also observed in methylated IBU, which cannot form H-bonds. It has been related to the analogous transformation of a methylated carboxyl group from the synperiplanar to the antiperiplanar conformation.[51] However, the amplitude of the process in Me-IBU is considerably smaller than that in normal IBU, which indicates that H-bonds strongly affect the D-process in nonmethylated IBU. By using MD simulations, Correia and Affuard found that although the synperiplanar to the antiperiplanar transformation of carboxyl groups in the H-bonded aggregates of IBU molecules is promoted by linear (single) H-bonds between IBU molecules, this transformation is hindered by cyclic (double) H-bonds between the O═C—O—H groups of IBU molecules.[50] Thus, the character of H-bonds formed between the same molecular species (IBU···IBU) and the different ones (IBU···acMAL) could be a hint on the occurrence of the D-process originated from the synperiplanar to the antiperiplanar transformation of carboxyl groups in IBU molecules in the IBU+acMAL mixtures. To gain a better insight into the properties of H-bonds that enable to form homodimers (IBU···IBU) and heterodimers (IBU···acMAL), we have performed calculations based on the density functional theory (DFT), details of which are described later in the paper. As a result, we have determined that the cyclic H-bonds between IBU and acMAL are stronger than those formed between two IBU molecules (see Figure 5). This conclusion can be drawn from the larger association energy of the heterodimer IBU···acMAL (ΔE_{ass} (IBU···acMAL) = 73.4 kJ/mol) than that of the homodimer IBU···IBU (ΔE_{ass} (IBU···IBU) = 66.6 kJ/mol). It suggests that the cyclic heterodimers IBU···acMAL may be easier formed than the cyclic homodimers IBU···IBU. Taking into account the results of DFT calculations as well as the observed position of s-process and the increase in its amplitude with increasing acMAL content (see Figure 3) in the case of the investigated binary mixtures, we suppose another effect of the cyclic H-bonds between different species, acMAL, and IBU molecules than those between IBU molecules on the synperiplanar to the antiperiplanar transformation of carboxyl groups in IBU molecules. It seems that the heterocyclic H-bonds may promote this transformation, which can be reflected in the s-process in dielectric spectra. Nevertheless, the presented scenario requires further investigations to its confirmation. As mentioned, the larger tendency to form the cyclic H-bonds between two different molecular species than those between two IBU molecules in the IBU+acMAL mixtures has been argued by exploiting our DFT calculations for two isolated molecules. For example, MD simulations of the binary IBU +acMAL mixtures would be useful to consider the effect of surrounding molecules on hydrogen bonding and to perform such statistical analysis of linear (single) and cyclic (double) H-bonds that enable the formation of homodimers (IBU···IBU) and heterodimers (IBU···acMAL), and consequently evaluate populations of molecular conformations, as it was carried out by Ottou Abe et al.[49] for hydrogen bonding in the case of pure ibuprofen and pure ketoprofen and their molecular conformations.

Nonisothermal Crystallization at $T > T_g$. On the basis of the dielectric study, we found that both the pure IBU and its binary mixtures with 5, 10, 20, and 30 wt % of acMAL are not physically stable and crystallize under nonisothermal conditions during their heating above T_g. As can be seen in Figure 2, the molecular mobility of investigated supercooled binary systems strongly depends on temperature (see Figure 2). When the sample is heated, both relaxation peaks (s- and α-) shift together to higher frequencies, which indicates that the time scale of molecular motions reflected in both relaxations

https://dx.doi.org/10.1021/acs.molpharmaceut.0c00517
Mol. Pharmaceutics 2020, 17, 3087−3105

becomes shorter with an increase in temperature. It should be noted that, at some temperature, a sudden drop in the amplitude of both s- and α-relaxation peaks occurs for all investigated systems due to a decreasing number of relaxing dipoles as a result of their immobilization during the crystallization process. The onset of the rapid decrease in the amplitude of structural relaxation indicates the beginning of the drug crystallization. Figure 2 shows that even 30 wt % of acMAL does not fully suppress IBU against the nonisothermal crystallization. It is interesting that the crystallization of all investigated systems occurs at a similar time scale of molecular mobility reflected in α-relaxation (i.e., $\tau_\alpha \sim 1.5\ \mu s$) regardless of acMAL content in the mixtures. It means that the global (structural) molecular mobility in the binary mixtures (IBU +acMAL) at such a characteristic time scale promotes the start of crystallization under nonisothermal conditions. However, it is clearly seen that temperatures of onset crystallization increase with increasing acMAL content, which may suggest that the physical stability of the systems with larger amounts of the excipient is improved. Since our binary systems differ in T_g, to properly estimate the degree of stability improvement of IBU by acMAL in the supercooled liquid state, we used the reduced crystallization temperature T_{red} as the normalized measure of the tendency to nonisothermal cold crystallization. The reduced crystallization temperature T_{red} has been defined by Zhou et al.[52] as the ratio of the temperature range between crystallization onset and glass transition ($T_{crystonset} - T_g$) to the temperature range between melting point and glass transition of a system ($T_m - T_g$):

$$T_{red} = \frac{T_{crystonset} - T_g}{T_m - T_g} \quad (1)$$

T_{red} can take values in the range from 0 to 1 and indicates how far above T_g the supercooled liquid may be heated before the cold crystallization occurs. If T_{red} tends to 1, the system is more resistant to the cold crystallization under nonisothermal conditions.

We found that T_{red} increases with increasing content of acMAL for IBU+acMAL systems, which indicates that acMAL gradually improves the physical stability of supercooled IBU in the binary mixture (see black stars in Figure 6). For concentrations of acMAL larger than $c_w > 10$ wt %, we observe a more rapid than linear growth of T_{red}, which suggests that the more effective stabilization of IBU begins from this concentration of acMAL. To assess the degree of the potential of acMAL to improve the physical stability of various drugs, we compare dependences of T_{red} as a function of the content of acMAL in binary mixtures with several pharmaceuticals: IBU, celecoxib (CEL), and nifedipine (NIF) (see Figure 6). From these plots, we evaluated crystallization parameters (CP) proposed by Bhugra et al.[53] within the range of small concentrations of the acMAL (0−10 wt %) in mixtures for which the dependences of T_{red} are linear (see Table 1). The values of CP (defined as the slopes of the linear fits) suggest that the potential of acMAL to retard the crystallization of drugs follows the rank order CEL > NIF > IBU.

Moreover, from Figure 6, it is clearly seen that values of T_{red} for the IBU+acMAL mixture (especially for smaller amounts of the excipient) are significantly smaller than those evaluated for CEL+acMAL and NIF+acMAL. It means that, among analyzed systems, the mixtures of IBU+acMAL are characterized by the weakest physical stability, whereas the mixtures of CEL

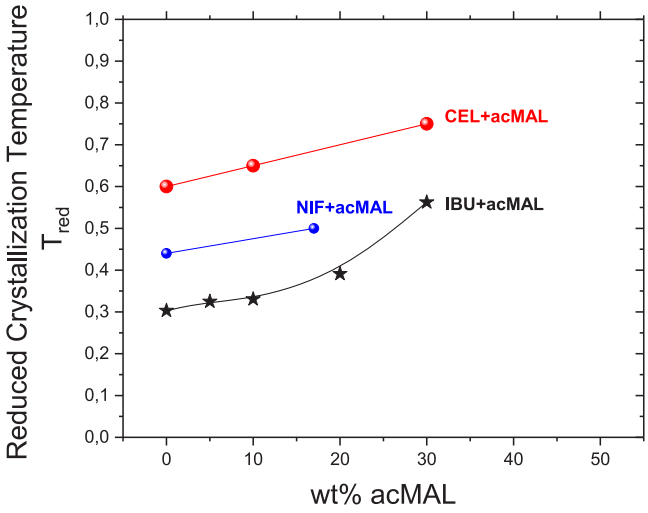

Figure 6. Reduced crystallization temperature T_{red} as a function of acMAL concentration in binary mixtures with different drugs: ibuprofen (black stars), celecoxib (red points), and nifedipine (blue points are calculated on the basis of data from ref 21).

Table 1. Values of the Crystallization Parameters CP and the Coefficients of Determination (R^2) for Binary Mixtures of Different Drugs (CEL, IBU, and NIF) with the Same Excipient (acMAL)

material	CP (slope of the linear fit)	R^2
CEL+acMAL	0.0050	1.0
NIF+acMAL	0.0035	1.0
IBU+acMAL	0.0027	0.9

+acMAL are the most resistant to the nonisothermal crystallization (the binary mixture of IBU with concentrations of acMAL larger than 30 wt % reaches the degree of the physical stability of pure CEL). The results of the analysis of T_{red} for investigated binary mixtures show that acMAL not very effectively acts as the crystallization inhibitor of IBU under nonisothermal conditions.

Isothermal Crystallization at $T > T_g$. In addition to nonisothermal crystallization investigations, the isothermal crystallization kinetics study of the pure supercooled IBU and its mixture with 10 wt % of acMAL at temperatures at which the systems have the same structural relaxation times, i.e., $\tau_\alpha \approx 2\ \mu s$ (see Figure 7a), were also carried out. If we have two systems which differ in T_g (like it is in the case of pure IBU and IBU+10 wt % acMAL), the crystallization time τ_{cryst} established for the same time scale of the global molecular mobility or the same viscosity of these systems seems to be the most appropriate measure of the tendency to isothermal crystallization of investigated systems. From the static dielectric permittivity collected during isothermal crystallization of both the systems (IBU and IBU+10 wt % acMAL) at the same structural relaxation time (see Figures 7b,c), we evaluated time dependences of the degree of crystallization (see Figure 7d). The increase in the crystallization degree with time is expressed by the normalized real permittivity ε'_N given by the following formula:

$$\varepsilon'_N(t) = \frac{\varepsilon'(0) - \varepsilon'(t)}{\varepsilon'(0) - \varepsilon'(\infty)} \quad (2)$$

https://dx.doi.org/10.1021/acs.molpharmaceut.0c00517
Mol. Pharmaceutics 2020, 17, 3087−3105

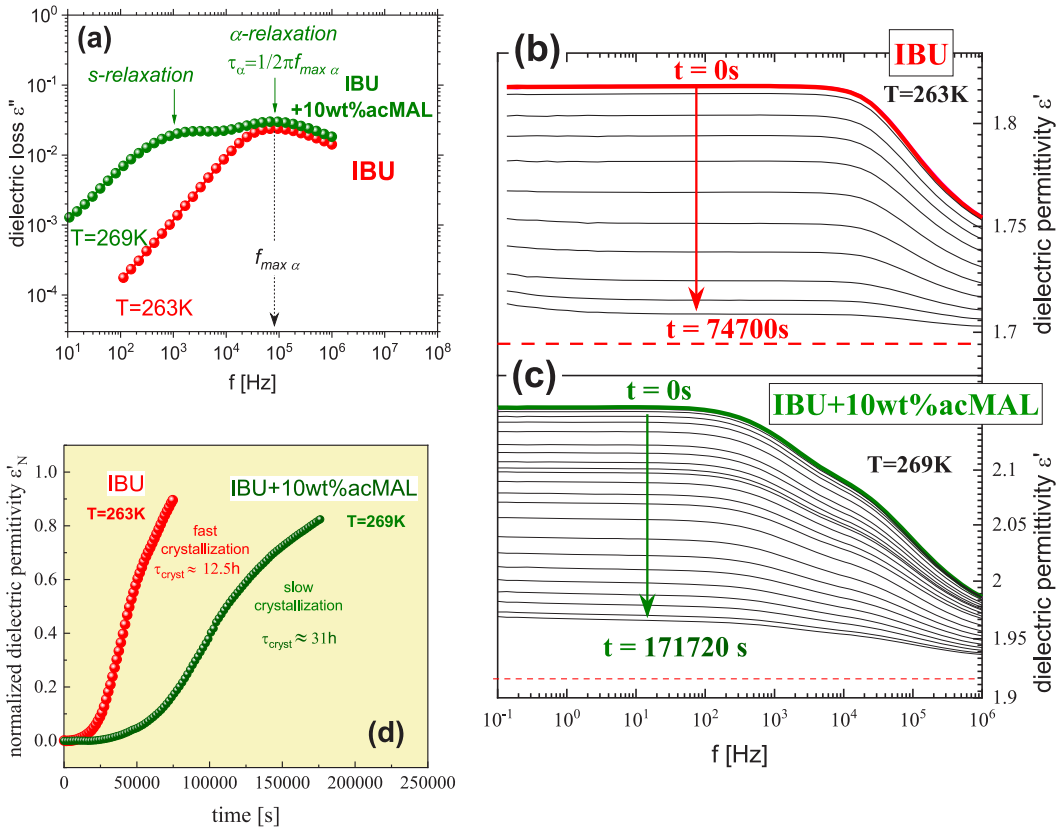

Figure 7. (a) Dielectric loss spectra for pure IBU and IBU+10 wt % acMAL obtained at temperatures 263 and 269 K, respectively, at which structural relaxation times for both systems are the same $\tau_\alpha = 2$ μs. Dielectric spectra of the real part of the complex dielectric permittivity collected during an isothermal crystallization of (b) pure IBU and (c) IBU+10 wt % acMAL at the same α-relaxation times $\tau_\alpha \approx 2$ μs. (d) Time dependence of normalized real permittivity ε'_N for pure IBU and its binary mixture IBU+10 wt % acMAL, obtained during the isothermal storage of these systems at different temperatures $T = 263$ K and $T = 269$ K, but at the same α-relaxation times $\tau_\alpha \approx 2$ μs for both of the systems.

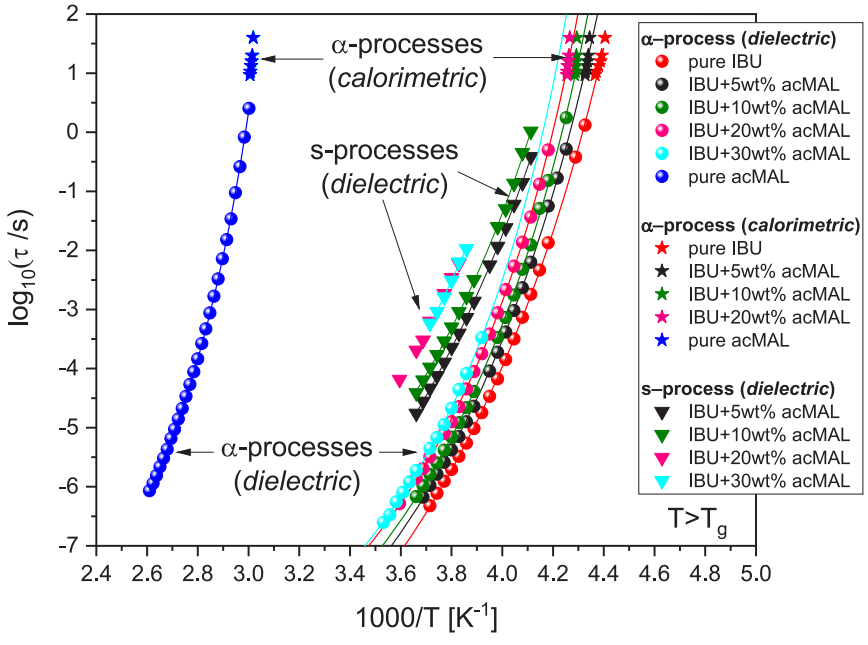

Figure 8. Relaxation map obtained at $T > T_g$ for pure IBU and pure acMAL and for their binary mixtures (IBU+acMAL) with different concentrations of acMAL. Circle and triangle points indicate the dielectric α- and s-relaxation times, respectively, whereas stars denote calorimetric α-relaxation times evaluated from TMDSC data.

where $\varepsilon'(0)$ is the static dielectric permittivity at the beginning of crystallization, $\varepsilon'(\infty)$ is the long-time limiting value of the dielectric permittivity, and $\varepsilon'(t)$ is the value of the dielectric permittivity at a given time of crystallization, t.

https://dx.doi.org/10.1021/acs.molpharmaceut.0c00517
Mol. Pharmaceutics 2020, 17, 3087−3105

From the crystallization kinetics curves presented in Figure 7d, we established that the crystallization process for IBU with 10 wt % acMAL is significantly longer than that for the pure drug. While the two systems have the same structural molecular mobility in the supercooled liquid state, the crystallization time of the mixture IBU+10 wt % acMAL is 18 h longer than that for neat IBU, which means that acMAL stabilizes IBU in the supercooled binary mixtures against the isothermal crystallization in isochronal conditions.

The enhancement of the physical stability of IBU by acMAL under isothermal and nonisothermal conditions can be related to H-bonds formed between IBU and acMAL molecules. Previous studies suggested that the cyclic H-bonds between IBU molecules favor the crystallization of the pure drug.[49] As already mentioned, acMAL molecules form stronger H-bonds with IBU molecules than those between molecules of the drug. Thus, we can suspect that the population of cyclic H-bonds between IBU molecules decreases at the expense of an increasing population of H-bonds between different molecular species in the binary mixtures (IBU+acMAL). In this way, the crystallization tendency of IBU is smaller due to the additive of acMAL.

Molecular Factors Determining Physical Stability at $T > T_g$. To obtain the relaxation map for all investigated systems, reflecting times scales of molecular motions in the wide temperature range, the complex permittivity $\varepsilon(\omega)$ of investigated mixtures has been described by means of the Havriliak–Negami (HN) formula:[54,55]

$$\varepsilon(\omega) = \varepsilon' - i\varepsilon'' = \varepsilon_\infty + \sum_k \frac{\Delta\varepsilon_k}{[1 + (i\omega\tau_k)^{\gamma_k}]^{\delta_k}} \quad (3)$$

where k indicates a relaxation process, $\Delta\varepsilon$ is the relaxation strength, τ is the HN relaxation time, γ and δ represent symmetric and asymmetric broadening of the loss curve, and ε_∞ is the high-frequency limit permittivity. When $\delta = 1$, the Cole–Cole (CC) function is generated. It should be noted that the shape of the s-relaxation peak in the binary mixtures is symmetrical but broad, and it cannot be described by the Debye formula (for which $\delta = 1$, $\gamma = 1$ in eq 3) like it was for the D-process in pure IBU. Therefore, dielectric spectra obtained for mixtures (at $T > T_g$) were fitted by means of the superposition of the HN (α-process) and the CC (s-process) functions. From this analysis of dielectric spectra, the relaxation maps for investigated systems above their T_g's were obtained (see Figure 8)

The temperature dependences of relaxation times for both the processes (α and s) are nonlinear and have been fitted to the Vogel–Fulcher–Tammann (VFT) formula:[56−58]

$$\tau_\alpha = \tau_\infty \exp\left(\frac{DT_0}{T - T_0}\right) \quad (4)$$

where τ_∞, T_0, and D are fitting parameters.

As can be seen in Figure 8, both the α- and s-processes rapidly slow down in the case of all examined systems during their vitrification. To identify which of them is indeed the structural relaxation related to the glass transition of the investigated binary systems, the stochastic temperature-modulated DSC study (TOPEM) has been performed. From the temperature and frequency dependences of the complex heat capacity, the calorimetric relaxation times as a function of temperature have been determined near T_g (see the star points in Figure 8). It is clearly seen that the faster process from dielectric measurements is certainly the structural α-relaxation of the binary mixtures because dielectric relaxation times of this process can be successfully extrapolated to the calorimetric α-relaxation times (calorimetric data lies along the VFT fit curve extrapolated from the dielectric data).

Antiplasticization. Based on the temperature dependences of the dielectric α-relaxation times, the values of the glass transition temperature T_g, defined at $\tau_\alpha(T_g)$ =100 s, were determined for all examined systems and plotted as a function of acMAL content in the binary mixtures and compared with those from DSC experiments. It is worth noting (see Figure 9) that the values of T_g from different experiments (i.e., dielectric, TMDSC, and standard DSC measurements) are approximately the same.

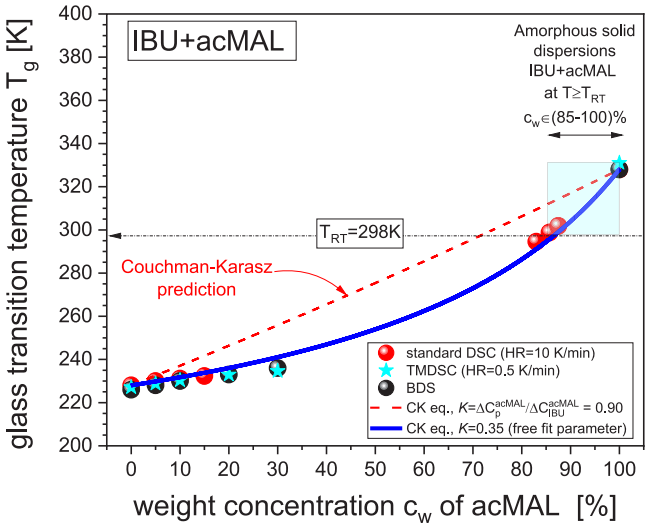

Figure 9. Plot of T_g values of the binary mixtures (IBU+acMAL) from dielectric and calorimetric measurements as a function of acMAL concentration. The red line indicates the fit curve of experimental data to eq 5 with the fixed-parameter $K = 0.90$ evaluated from DSC data, whereas the blue line shows the free fit curve of the experimental data to eq 5 for which the parameter $K = 0.35$ deviates significantly from that determined from DSC.

The enhancement of the physical stability of IBU by acMAL in the supercooled binary mixtures is associated with some antiplasticization effect of the excipient on IBU, which is the consequence of the slowdown in the global molecular mobility of these systems. However, as can be seen in Figure 9, the increase in T_g of binary mixtures with adding acMAL is much weaker than the Couchman and Karasz (CK) prediction:[59]

$$T_g = \frac{w_{IBU}T_{gIBU} + Kw_{acMAL}T_{gacMAL}}{w_{IBU} + Kw_{acMAL}} \quad (5)$$

where w_{IBU} and w_{acMAL} are the mass fractions of each component and T_{gIBU} and T_{gacMAL} are their corresponding T_g values. The constant K in the CK model (eq 5) is related to the ratio of the change in heat capacity at T_g of the two components of investigated binary mixtures ($K = \Delta C_{pacMAL}/\Delta C_{pIBU}$). For IBU+acMAL mixtures, the parameter $K = 0.90$ was determined using values of $\Delta C_{p\_acMAL} = 0.38$ J/(gK) and $\Delta C_{p\_IBU} = 0.42$ J/(gK) measured by TOPEM.

The experimental dependence of T_g vs acMAL concentration (blue line in Figure 9) described by the CK equation with the free fitting parameter $K = 0.35$ shows a negative

https://dx.doi.org/10.1021/acs.molpharmaceut.0c00517
Mol. Pharmaceutics 2020, 17, 3087−3105

deviation from the CK prediction (red line in Figure 9) that assumes an ideal mixing. An analogous pattern of the behavior of T_g vs content of mixture components for different binary systems has been thoroughly analyzed by Shamblin et al.[60] They have argued that such a deviation from the CK prediction (due to the experimental T_g values lower than the expected ones) occurs if the total energy of interactions between molecules of different molecular species is less than that between molecules of the same molecular species. In case of mixtures containing some polymer blends, the authors considered that the decrease in T_g below the CK curve can be caused by a net loss in the degree of hydrogen bonding on mixing, which means the fewer number and/or strength H-bonds between molecules of different molecular species relative to the H-bonds between molecules of the same molecular species. In the case of the investigated binary mixtures (IBU+acMAL), H-bonds formed between IBU and acMAL molecules should be stronger than those formed between two IBU molecules, as we have already discussed herein based on our DFT calculations. Thus, the negative deviation from the CK prediction for IBU+acMAL mixtures may indicate that there are some steric constraints caused by acMAL molecules in the binary mixtures, which hinder the formation of H-bonds between IBU molecules, and/or the strength of H-bonds formed between IBU and acMAL molecules may slightly weaken, if a molecule of acMAL accepts a few IBU molecules, whereas the contribution of van der Waals interactions between acMAL molecules to molecular dynamics of the binary mixtures increases. It is worth noting that the number of H-bonds formed between IBU and acMAL molecules reaches a saturation level at which almost all IBU molecules are hydrogen bonded by acMAL molecules. Invoking our DFT calculations, one can assume that the saturation level for hydrogen bonds in the IBU+acMAL systems is characterized by three or even four H-bonds effectively formed by each acMAL with IBU molecules, which corresponds to the mole fraction of acMAL $x_w \approx 0.2$. Then, the increasing acMAL content in the binary mixtures (IBU +acMAL) results in a gradually dominating role of van der Waals interactions between acMAL molecules in the systems.

Moreover, from Figure 9, one can see some disadvantages of IBU+acMAL binary systems from the application point of view. To obtain the amorphous solid dispersion (ASD) of IBU +acMAL at room temperature T_{RT}, a large content of acMAL excipient (more than >85 wt %) is necessary. Binary mixtures of IBU with smaller content of acMAL than 85 wt % are not solid at T_{RT} but very viscous liquids. Due to the need to use a large concentration of acMAL for ASD preparation, acMAL is not the best candidate that could give a satisfactory formulation for IBU.

Fragility. Another factor associated with the temperature dependences of the global molecular mobility and very often used to predict the physical stability of amorphous systems is isobaric fragility parameter m_p defined by the following formula:

$$m_p = \left.\frac{d\log\tau_\alpha}{d(T_g/T)}\right|_{T=T_g} \quad (6)$$

The fragility parameter is closely related to the apparent activation energy for α-relaxation ΔE_a determined at T_g, $m_p = \Delta E_a(T_g)/T_g$, where R is the gas constant and ΔE_a is defined[61] at a constant pressure as follows:

$$\Delta E_a(T) = R\frac{d\ln\tau_\alpha}{d(1/T)} \quad (7)$$

The fragile liquids are characterized by a higher ratio $\Delta E_a(T_g)/T_g$ in comparison with strong materials. The fragility parameter is a measure of the sensitivity of molecular dynamics of supercooled liquids to changes in temperature near the glass transition. In terms of the value of m_p, glass-forming liquids are classified as strong ($m_p \leq 30$), moderately fragile ($30 < m_p < 100$), and fragile ($m_p \geq 100$). A large value of m_p indicates that small temperature fluctuations near T_g cause significant changes in molecular mobility that may lead to stable nuclei or to attach to a growing crystal face, which is the reason for a large tendency of material crystallization. Therefore, it is regarded that more fragile drugs have a larger tendency to crystallize, whereas the physical stability is better for stronger liquids (i.e., for smaller values of m_p) in both the supercooled liquid and glassy states. However, there are known exceptions for this correlation for pure drugs.[62−64] Although most drugs are classified as fragile or moderately fragile, these systems nevertheless are characterized by a completely different tendency to crystallization.

Recently, we have tested whether this correlation is fulfilled for some binary systems. We have found that the better physical stability correlates with the decrease in the fragility parameter with increasing content of excipient in a mixture for CEL+acMAL and CEL+PVP binary systems.[20] A similar correlation has also been reported for the binary mixtures of indomethacin (IND) with acMAL[22] (see Figure 10a).

In the case of the IBU+acMAL binary mixtures examined here, we have established the opposite correlation of fragility with the physical stability of the systems. As can be seen in Figure 10a, the fragility parameter for IBU+acMAL significantly increases with increasing content of the excipient in the mixture despite the increasing improvement of IBU stability in the binary systems. It is worth noting that Kaminska and co-workers also found such an opposite correlation for binary mixtures of nifedipine with several acetylated saccharides.[21] This indicates that the fragility parameter does not always correctly predict the stability of amorphous drugs. Thus, we cannot recommend the use of the fragility parameter to predict the tendency of drugs to crystallization.

Activation Energy of α-Relaxation. In addition to the fragility parameter, the activation energy is one of the most fundamental characteristics of structural relaxation and glass transition. Therefore, we checked whether the activation energy E_a of the α-relaxation determined at T_g of IBU +acMAL and CEL+acMAL binary mixtures also exhibits different patterns of behavior as a function of the molar fraction of the excipient (see Figure 10b). Molecular rearrangements reflected in structural relaxation need some amount of activation energy E_a to overcome the thermodynamic potential barriers. Thus, this dynamic factor can be helpful in the study of the physical stability of amorphous drugs. As can be seen in Figure 10b, the dependences of the activation energy for IBU+acMAL and CEL+acMAL vs the molar fraction x_w of acMAL reveal a similar pattern of behavior as we found for m_p. It is very interesting that the dependence for IBU+acMAL monotonically increases from very small values of E_a with increasing content of acMAL, whereas the

https://dx.doi.org/10.1021/acs.molpharmaceut.0c00517
Mol. Pharmaceutics 2020, 17, 3087−3105

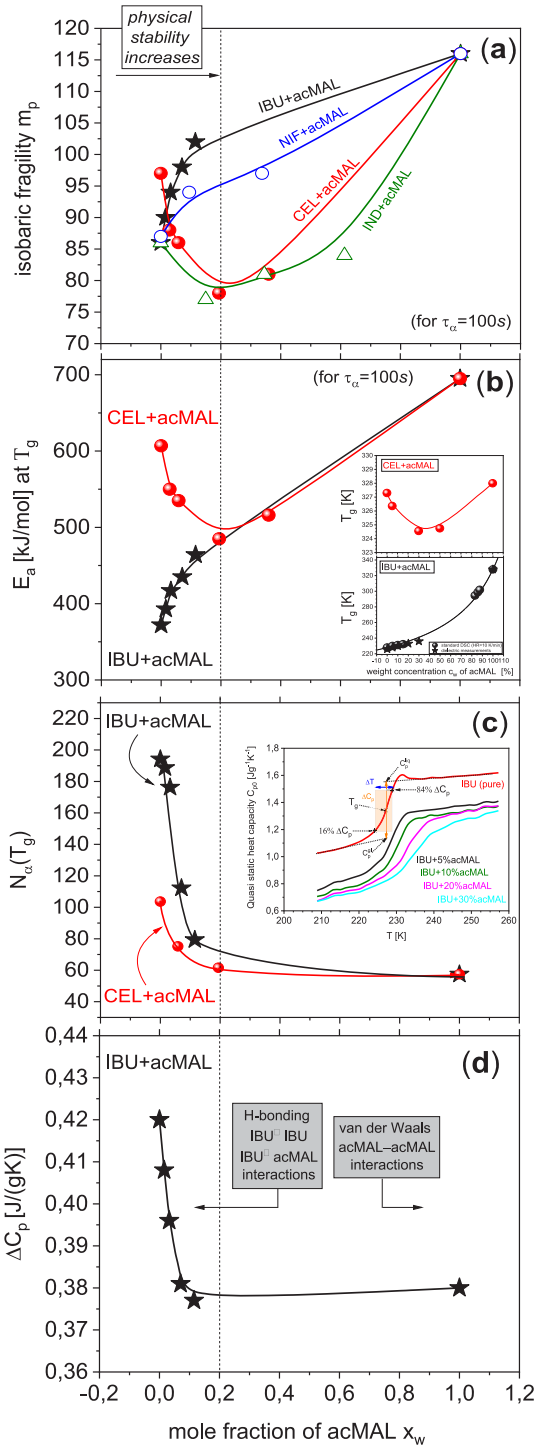

Figure 10. Dependences of acMAL mole fraction on different molecular factors for binary mixtures (drug+acMAL): (a) isobaric fragilities (data for binary mixtures indomethacin (IND), nifedipine (NIF), and celecoxib (CEL) with acMAL were taken from refs 22, 21, and 10, respectively), (b) activation energy E_a of dielectric α-relaxation at T_g of the binary systems (the inset shows glass transition temperatures for IBU+acMAL and CEL+acMAL as a function of weight concentration of acMAL), (c) numbers of dynamically correlated molecules N_α at T_g evaluated from Donth model (eq 8) based on temperature dependences of the heat capacity C_p of investigated systems showed in the inset, (d) the change in the heat capacity ΔC_p at T_g of investigated systems of IBU+acMAL derived from data showed in the inset of panel c.

function of E_a (x_w) for CEL+acMAL is nonmonotonic (initially, the addition of acMAL to CEL results in a decrease in E_a of the binary mixture, whereas the values of E_a become increasing for $x_w > 0.2$). The values of E_a for pure drugs (IBU and CEL) differ significantly (by around 300 kJ/mol), but they converge and become nearly the same for $x_w > 0.2$. These findings for m_p and E_a are intriguing because molecular interactions in both the binary systems are similar: molecules of pure drugs can form H-bonds (IBU···IBU and CEL···CEL), as well as molecules of drugs, and may form H-bonds with the excipient molecules (IBU···acMAL and CEL···acMAL), whereas only van der Waals interactions are relevant between molecules of acMAL. It indicates that H-bonded supramolecular structures are different in both the binary systems, which influences their global molecular dynamics. We have also observed that the dependences of the activation energy E_a at T_g on the acMAL content in the binary mixtures correlate with the plasticization/antiplasticization effects of the excipient on the drugs (IBU and CEL). Small amounts of acMAL plasticize CEL (see the upper inset in Figure 10b); that is, the molecular mobility reflected in the structural relaxation of the CEL+acMAL mixture at T_g increases, which corresponds to the decrease in E_a of the global relaxation. On the contrary, above 30 wt % of acMAL in the CEL+acMAL mixture, the antiplasticization effect is observed; that is, the structural molecular mobility begins to grow, which is correlated with the increase in E_a at T_g. However, in the case of the IBU+acMAL binary system, acMAL exerts only an antiplasticization effect on IBU for any content of the excipient (see the lower inset in Figure 10b), which is reflected in the monotonic growth of E_a with adding acMAL to IBU.

Dynamic Heterogeneity. One of the fundamental problems is how different kinds of molecular interactions affect the dynamic heterogeneity of the global molecular dynamics of the supercooled liquids and, consequently, their physical stability?

The concept of dynamic heterogeneity has been firmly established in the glass transition physics since 1965, when the Adam–Gibbs model was formulated.[65] Within this model, the molecular mobility near the glass transition is characterized by correlated motions of neighboring molecules, which results in the appearance of cooperatively rearranging regions (CRR) defined as a subsystem that can rearrange into another configuration independently of its environment upon a sufficient thermal fluctuation.[66] Hence, the rapid slowdown in molecular dynamics observed near the glass transition has been attributed to an increasing size of CRRs, reflecting that the molecular dynamics of a supercooled liquid becomes more and more heterogeneous in both time and space domains when approaching the glass transition. The experimental and evaluation ways to find a characteristic number of dynamically correlated molecules N_α, which determines the characteristic size of dynamic heterogeneity, are still debated.[67] Since direct measurements of N_α are very difficult, various estimates are applied to quantify N_α. Among them, the commonly used ones are the estimates based on the fluctuation–dissipation theorem, which have been proposed separately for the entropy fluctuations by Donth[68,69] and the enthalpy fluctuations by Berthier et al.[70] In contrast to the latter, the Donth estimate requires experimental data collected only by using a single measurement technique that provides a temperature dependence of the specific heat capacity C_p measured within the temperature range in which the glass transition occurs. The width of the step in the temperature dependence $C_p(T)$ at the

https://dx.doi.org/10.1021/acs.molpharmaceut.0c00517
Mol. Pharmaceutics 2020, 17, 3087–3105

glass transition has been related to the size of temperature fluctuations.[71] Consequently, the number of dynamically correlated particles, $N_\alpha(T_g)$, or the corresponding volume of the area occupied by the dynamically correlated molecules, $V_\alpha(T_g) = N_\alpha(T_g)/\rho$, can be estimated by the following equation:

$$N_\alpha(T_g) = \frac{N_A\left(\frac{1}{C_p^{glass} - C_p^{liquid}}\right)}{M(\delta T)^2} k_B T_g^2 \quad (8)$$

where T_g is the glass transition temperature, ρ is the material density, k_B is the Boltzmann constant, M is the molar mass, C_p^{glass} and C_p^{liquid} are the isobaric heat capacities of glass and liquid at T_g, and δT is the average temperature fluctuation, which is related to the dynamic glass transition. The Donth formula was originally derived[68] in the NVT statistical ensemble. However, eq 8 is its representation in the NPT statistical ensemble,[72] which is suitable to use in typical experimental conditions.

We have applied the Donth model to determine the number of dynamically correlated molecules at T_g, exploiting the results of TOPEM measurements for pure compounds (IBU, CEL, and acMAL) and for investigated binary systems (IBU+acMAL and CEL+acMAL) with different content of acMAL. To our best knowledge, such analyses of the dynamic heterogeneity have not been made in mixtures until now. As can be seen in Figure 10c, in contrast to the activation energy and fragility of the binary systems (IBU+acMAL and CEL+acMAL), the number of dynamically correlated molecules N_α rapidly decreases with increasing acMAL content in the entire range of acMAL mole fraction x_w.

The dramatic decreasing dependences $N_\alpha(x_w)$ reflect the already discussed changes in the character of molecular interactions from H-bonded to van der Waals systems when adding acMAL to both the drugs. The numbers of dynamically correlated molecules drop from the largest values for H-bonded pure drugs to the smallest one for acMAL interacting via van der Waals forces. It should be noted that N_α for IBU is larger than that for pure CEL (195 and 105 molecules, respectively). It is probably related to the more complex H-bonding rearrangements in the case of pure IBU compared to pure CEL or/and the stronger H bonds formed between IBU molecules than those between CEL molecules (as established from our DFT calculations performed herein for IBU systems and previously for CEL systems).[10] All findings depicted in Figure 10c seem to be significant to the glass transition physics because they suggest that there is a correlation between N_α and changes in the H-bonded supramolecular structures in the system, which requires, however, further investigations of other H-bonded systems to verify whether it is a rule or not. This issue is very interesting, especially since a similar rapid decrease in N_α due to the changing character of intermolecular interactions from supercooled liquids dominated by dipole–dipole interactions to their counterparts dominated by ionic interactions has been recently established from the comparative analysis of selected drugs formed as bases and their protic ionic counterparts.[73]

It should be emphasized that the Donth method enables the evaluation of the dynamic property N_α only based on thermodynamic parameters (eq 8). One of them is the jump in the heat capacity ΔC_p at T_g, which reflects a change in molecular mobility during the glass transition. It is interesting that ΔC_p rapidly decreases when adding acMAL to IBU similarly to N_α (see Figure 10d). It suggests that the change of some molecular motions related to the jump of the heat capacity ΔC_p during the glass transition is larger for systems with H-bonded supramolecular structures than that for van der Waals glass-forming liquids.

It is very tempting to find a correlation between N_α and the tendency to crystallization. Such attempts have been earlier made for some simulation models[74−76] and a few neat drugs.[77,78] For neat sildenafil, it has been found that the improvement of physical stability is correlated with an increase in N_α. In the case of the compared binary systems (IBU +acMAL and CEL+acMAL), we obtained the opposite dependence; i.e., N_α, as well as the tendency to crystallization, decreases when adding acMAL to the drugs (in the range $0 < x_w < 0.2$). Although it has been suggested that a net loss in hydrogen bonding occurs when adding acMAL to the mixtures, which seems to be revealed in the drop in N_α, we need to remember that the population of H-bonded heteroclusters (IBU···acMAL, and CEL···acMAL) increases at the expense of H-bonded homoclusters of medicines (IBU···IBU and CEL···CEL) up to a saturation level at which almost all drug molecules are hydrogen bonded by acMAL molecules (at $x_w \approx 0.2$). The formation of such H-bonded supramolecular heterostructures is considered in both the binary mixtures IBU+acMAL and CEL+acMAL as a molecular mechanism, improving the physical stability of the systems. However, N_α reflects the average dynamic heterogeneity of a binary mixture coming from H-bonded homoclusters, H-bonded heteroclusters, and van der Waals interactions. Thus, we are not able to distinguish the contribution to the dynamic heterogeneity coming from only such H-bonded heterostructures, improving the physical stability of the drugs in the binary mixtures with acMAL. Nevertheless, we can suppose that the population of H-bonded heteroclusters, which increases relative to the population of H-bonded homoclusters (with increasing content of acMAL in the range $0 < x_w < 0.2$), should result in a relative increase in the number of dynamically correlated molecules involved in the H-bonded heteroclusters, and this increase could be relevant to the improvement of the physical stability of the binary mixtures.

Relaxation Processes at $T < T_g$. It has been often considered that local molecular motions reflected in secondary relaxations can be responsible for nucleation and consequently crystallization of drugs in the glassy state.[16,79,80] The secondary processes are typically classified into Johari−Goldstein (JG) and non-JG relaxations. The JG relaxation has a local intermolecular character (small-angle rotations of entire molecules) and is regarded as a precursor of the molecular mobility of the cooperative α-relaxation, whereas non-JG relaxations reflect some intramolecular motions of some parts of molecules.[81] Secondary relaxations of pure IBU have already been thoroughly analyzed both under ambient and elevated pressure.[48,47] It has been found that pure IBU exhibits two secondary relaxations (β and γ). The fast γ-process of pure IBU is insensitive to pressure changes, and it was classified as an intramolecular non-JG relaxation.[48] Whereas the slower β-relaxation has been assessed as the local intermolecular JG process based on the Coupling Model analysis,[47] which has been later confirmed by finding its sensitivity to pressure changes.[48] However, pure acMAL exhibits only one secondary relaxation, called the μ-process, which originates from the

https://dx.doi.org/10.1021/acs.molpharmaceut.0c00517
Mol. Pharmaceutics 2020, 17, 3087−3105

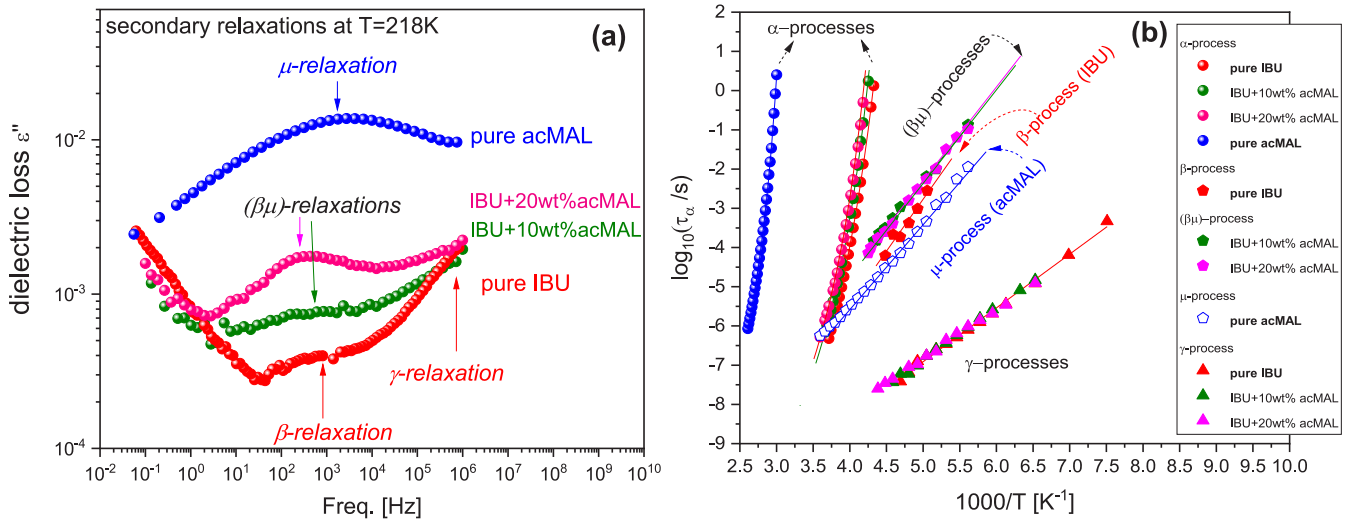

Figure 11. (a) Comparison of dielectric spectra for pure IBU, acMAL, and binary mixtures of IBU with acMAL obtained in the glassy state of investigated systems at the same temperature (218 K) at which secondary relaxations are observed. (b) Temperature dependences of structural (α) and secondary (β, ($\beta\mu$), μ, and γ) relaxations times for pure IBU, acMAL, and binary mixtures of IBU with acMAL.

intramolecular rotations of the acetyl moiety (C−O−($COCH_3$)) in the acMAL molecule.[10]

As can be seen in Figure 11a, the μ-process of pure acMAL and the β-process of pure IBU are observed within the same frequency range, but the μ-process of the excipients has a considerably larger magnitude than the β-relaxation of the drug. Consequently, when acMAL is added to IBU, we observe a significant increase in the contribution of the μ-process to dielectric spectra of the binary mixtures. The magnitude of the ($\beta\mu$)-process in the binary mixtures, which is a superposition of β- and μ-processes of the pure compounds, increases with an increasing amount of acMAL in the mixture. It indicates that the molecular dynamics of mixtures in the glassy state is gradually dominated by acMAL. Nevertheless, the significant increase in the dielectric strength of the ($\beta\mu$)-process is accompanied by only a slight slowdown in the relaxation and a small decrease in its activation energy when adding acMAL to the drug (see Figure 11b in which dielectric loss spectra are shown at T = 218 K as a representative example and Table 2). Therefore, the molecular motions reflected in the JG relaxation do not seem to influence the physical stability of the IBU +acMAL binary mixtures.

Analyzing the non-JG γ-process in IBU, we have found that its dielectric strength is nearly invariable when adding acMAL to the drug. The insensitivity of the γ-relaxation to acMAL is also represented by the same values of the activation energy and relaxation times for the γ-process in pure IBU and its binary mixtures with acMAL (see Figure 11b and Table 2).

Table 2. Values of the Activation Energy of Secondary Relaxations Observed in Pure IBU, acMAL, and Binary Mixtures IBU+acMAL Derived Using the Arrhenius Law

material	ΔE_β [kJ/mol]	$\Delta E_{(\beta\mu)}$ [kJ/mol]	ΔE_μ [kJ/mol]	ΔE_γ [kJ/mol]
pure IBU	51			26
IBU+10% acMAL		44		26
IBU+20% acMAL		44		26
pure acMAL			41	

Thus, we should exclude any role of the γ-relaxation in the enhancement of the physical stability of IBU by mixing with acMAL. To find the origin of the intramolecular dielectric γ-process in IBU, we have performed DFT calculations for the drug molecule. In the DFT simulation, we have considered four different intramolecular rotations in the IBU molecule: Ph−C_2H_4COOH (Φ_1), Ph−$CH_2C_3H_7$ (Φ_2), PhC_2H_4−COOH (Φ_3), $PhCH_2$−C_3H_7 (Φ_4) presented in Figure 12a. The energy and dipole moment changes of IBU molecule as a function of rotation angles Φ_1, Φ_2, Φ_3, and Φ_4 are shown in Figure 12b−e, respectively. On the basis of the DFT analyses, we have established that the rotation around the axis $PhCH_2$−C_3H_7 with respect to the angle Φ_4 has the highest activation energy (ΔE = 21 kJ/mol) among all the examined intramolecular rotations. This value is close to the activation energy (ΔE_γ = 26 kJ/mol) of the γ-relaxation, which suggests that the secondary dielectric process originates from the $PhCH_2$−C_3H_7 reorientations. It is worth noting that the rotation $PhCH_2$−C_3H_7 reflected in the γ-relaxation (not involved in improving the physical stability of IBU) cannot be affected by hydrogen bonding. It reinforces our previous consideration of the important role of H-bonds dynamics in reducing the tendency of IBU to crystallization in the binary systems with acMAL.

WATER SOLUBILITY AND DISSOLUTION RATE STUDY

Finally, we studied the water solubility and the dissolution rate of IBU in the binary systems with large amounts of acMAL, which are amorphous solid dispersions (ASDs) in normal conditions. The solubility of the drug was tested in distilled water at room temperature. The equilibrium solubilities have been measured after 48 h. We found that although acMAL improves the physical stability of amorphous IBU in the binary mixtures, it does not significantly improve the solubility of the drug in water from the ASDs. The equilibrium water solubility of IBU from ASD with the large contents of acMAL (IBU+83 wt % acMAL, IBU+86 wt % acMAL, and IBU+87.5 wt % acMAL) is only ∼10% higher in comparison with the water solubility of the pure crystalline IBU (see Figure 13). It should be noted that the IBU mixtures with small acMAL content,

https://dx.doi.org/10.1021/acs.molpharmaceut.0c00517
Mol. Pharmaceutics 2020, 17, 3087−3105

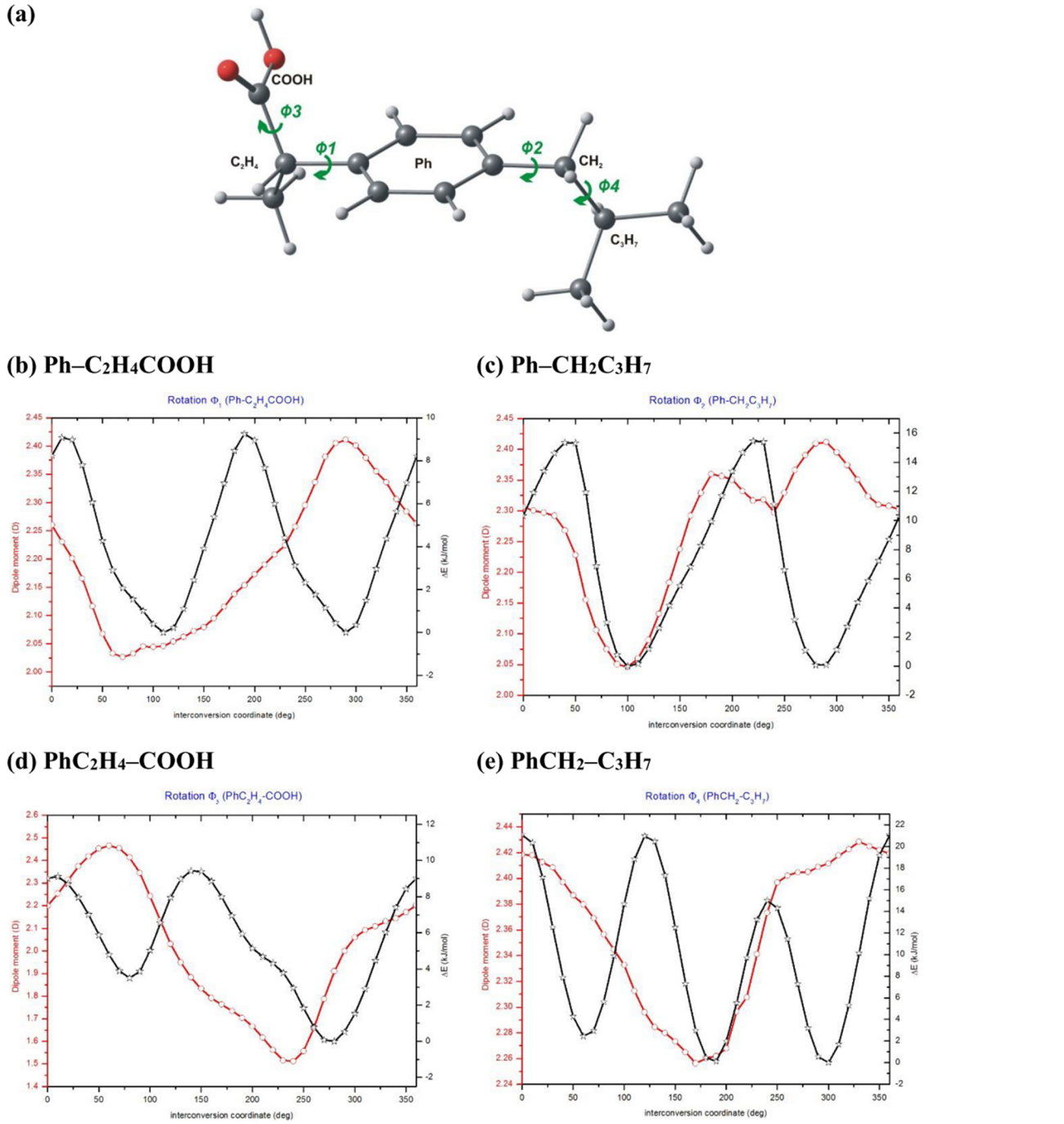

Figure 12. (a) Molecular structure of ibuprofen monomer. Geometry of structures optimized at the DFT/B3LYP/Def2-TZVP level of theory. Rotation coordinates are depicted: Φ_1, Φ_2, Φ_3, and Φ_4. (b–e) Energy (black line) and dipole moment changes (red line) of ibuprofen molecule as a function of rotation angle Φ_1, Φ_2, Φ_3, and Φ_4, respectively.

which are supercooled viscous liquid at room temperature, immediately recrystallized during the contact with water.

Additionally, we analyzed the dissolution profiles of IBU from ASD with the large contents of acMAL (i.e., for IBU+83 wt % acMAL, IBU+86 wt % acMAL, and IBU+87.5 wt % acMAL) in the water at a human body temperature (37 °C). We observed that the dissolution rate of pure crystalline IBU is much higher than that for ASD with acMAL. It indicates that acMAL negatively affects IBU, significantly retarding the rate of release of the drug from ASD (Figure 14).

These results are interesting because there are several examples of drugs (e.g., celecoxib[10] and indomethacine[22]) for which the water solubility considerably is improved by acMAL in ASD. However, these drugs are characterized by much higher values of T_g than that of IBU, and consequently, the values of T_g of their ASDs with acMAL are higher than 40 °C. Whereas in the case of ASD of IBU with acMAL, despite the huge content of acetylmaltose in the ASDs, the values of T_g of the binary mixtures of IBU with acMAL are very low, close to room temperature (see Figure 9). The poor dissolution rate of the ASD of IBU with acMAL is probably associated with the

https://dx.doi.org/10.1021/acs.molpharmaceut.0c00517
Mol. Pharmaceutics 2020, 17, 3087–3105

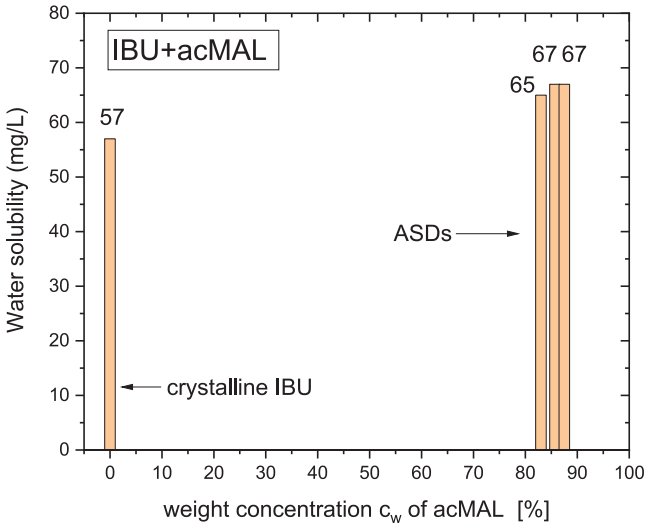

Figure 13. Equilibrium water solubilities of the pure crystalline IBU and amorphous IBU in ASDs with large contents of acMAL (i.e., for IBU+83 wt % acMAL, IBU+86 wt % acMAL, and IBU+87.5 wt % acMAL) at room temperature.

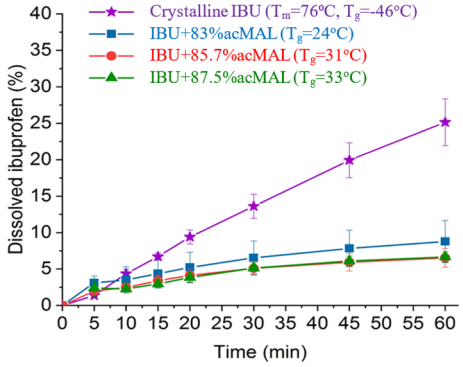

Figure 14. Dissolution profiles in water for the pure crystalline IBU and amorphous IBU from ASDs with various amounts of acMAL at 37 °C.

fact that the temperature of the dissolution medium (i.e., water) was higher (like the temperature of the human body) than T_g of all of the tested systems. Consequently, the binary mixtures (IBU+acMAL) at a human body temperature become rubbery and stuck into agglomerates of limited surface area, reducing their dissolution rate in water. Therefore, we recommend formulating the ASDs of much higher T_g than the temperature of the human body (ca. 37 °C) to avoid some agglomerations of sticky particles prior to starting dissolution.

CONCLUSIONS

Two dielectric processes (i.e., the slow s-relaxation and α-structural relaxation) have been observed above T_g of the binary mixtures IBU+acMAL. Nevertheless, our study has not confirmed any inhomogeneity and microphase separation of the investigated binary systems. The amplitude of the s-process increases rapidly with increasing content of acMAL in the mixture in a much more intensive manner than the α-structural relaxation peak. After considering the dielectric behavior of the s-process, our DFT calculations, and earlier published reports on neat IBU, we suppose that the origin of s-process may come from the synperiplanar to the antiperiplanar transformation of carboxyl groups in IBU molecules, which is possibly promoted by heterocyclic H-bonds between IBU and acMAL molecules, but this scenario requires further investigations to its confirmation.

Based on isothermal and nonisothermal crystallization investigations, we have found that acMAL improves the physical stability of supercooled IBU, which has a big tendency to crystallize above T_g as a pure compound. However, we have evaluated that the stabilization effectiveness of acMAL is less for IBU than that for celecoxib or nifedipine. The enhancement of physical stability of IBU in the binary systems with acMAL is due to interplaying mainly two factors: specific intermolecular interactions between IBU and acMAL by strong H-bonds and some antiplasticization effect of acMAL on IBU. Heteroclusters formed by IBU and acMAL molecules through H-bonds hinder the formation of double H-bonds between IBU molecules and consequently prevent the drug crystallization. The glass transition temperature T_g of the binary mixtures increases with adding acMAL. However, this antiplasticization effect, related to the slowdown in the global molecular mobility, is much weaker than that predicted by the Couchman−Karasz equation. It can affect stabilization effectiveness. The negative deviation of the experimental dependence of T_g on the content of acMAL from the CK prediction can be caused by a net loss of hydrogen bonding, suspected in the tested binary systems when adding this excipient.

We have also examined other important parameters often considered as molecular factors of the tendency to crystallization such as the fragility parameter m_p, the activation energy for structural relaxation E_a, and the average number of dynamically correlated molecules, quantifying the dynamic heterogeneity of the investigated systems, N_α. The thorough analyses of the parameters m_p, E_a, and N_α, evaluated at the glass transition temperatures of the binary mixtures of IBU with acMAL have enabled us to formulate a few observations on the utility of these parameters to predict the physical stability of the binary pharmaceutical systems with acMAL. (i) We have established that the fragility parameter inversely correlates with the crystallization tendency of the IBU+acMAL binary mixtures, which is opposite to the expected correlation. Thus, we cannot recommend the fragility to use as a universal parameter to predict the tendency of drugs to crystallization. (ii) The dependence of the activation energy E_a for structural relaxation at T_g on the content of acMAL in the binary mixtures is qualitatively the same as that for m_p and exhibit different monotonicities for two kinds of binary systems (IBU +acMAL) and (CEL+acMAL). For these reasons, none of these parameters can be exploited separately as a reliable factor of the physical stability of the amorphous pharmaceutical systems. However, we have found that the changes in m_p and E_a correlate with the plasticization/antiplasticization effects of acMAL on the drugs (IBU and CEL). (iii) Only the dependence of the dynamically correlated molecules N_α on the content of acMAL x_w has the same monotonicity in both kinds of binary mixtures (IBU+acMAL) and (CEL+acMAL). The decreasing dependences $N_\alpha(x_w)$ can be caused by changes in the character of intermolecular interactions in these binary systems with increasing acMAL content, which transform the initially strongly H-bonded supramolecular structures to the systems dominated by van der Waals interactions. This finding seems to be significant to the glass transition physics and requires further verifications by studying other H-bonded systems. However, a straightforward correlation between the

https://dx.doi.org/10.1021/acs.molpharmaceut.0c00517
Mol. Pharmaceutics 2020, 17, 3087−3105

physical stability and the dynamic heterogeneity quantified by N_α cannot be established because the estimate of N_α reflects the average dynamic heterogeneity of the binary mixture coming from H-bonded homoclusters (API···API), H-bonded heteroclusters (API···acMAL), and van der Waals interactions, whereas the improvement of the drug physical stability by acMAL is mainly associated with the formation of heteroclusters (API···acMAL).

Comparing the secondary relaxation processes in pure IBU and its binary mixtures with acMAL in the glassy state, we have found that the activation energy and the relaxation times of the JG process only slightly vary when adding acMAL to the drug, and these quantities are even invariant in the case of the non-JG relaxation. Thus, the molecular motions reflected in the JG ($\beta\mu$)- and non-JG γ-processes observed in the glassy state of the IBU+acMAL mixtures do not seem to influence the physical stability of these binary systems.

Our study of the water solubility as well as the dissolution rate of IBU in the binary systems with a large amount of acMAL, which form amorphous solid dispersions (ASDs) in normal conditions, has revealed that acMAL unfavorably affects these properties of IBU. The water solubility of such ASDs at room temperature is slightly improved compared to pure crystalline IBU, and acMAL significantly retards the release rate of the drug from ASDs at human body temperatures. The latter negative effect is most probably caused by forming some agglomerations of sticky particles prior to starting dissolution. To avoid such inconveniences, we may recommend that T_g of ASDs should be much higher than the human body temperature.

Our research shows that acMAL is not a universal excipient for any amorphous API that improves its properties. The binary compositions of IBU and acMAL examined herein in the supercooled liquid and glassy states are the first examples of the application of acMAL to stabilize the ASDs, which are not recommended to use due to their poor water solubility and dissolution rate as well as relatively small stabilization effectiveness. Nevertheless, this case provides us with valuable advice on how one should combine drugs and their crystallization inhibitors to prepare physically stable ASDs characterized by a better water solubility and dissolution rate in the therapeutically relevant temperature range.

AUTHOR INFORMATION

Corresponding Author

Katarzyna Grzybowska − *Institute of Physics, University of Silesia in Katowice, 41-500 Chorzów, Poland; Silesian Center for Education and Interdisciplinary Research, 41-500 Chorzów, Poland;* orcid.org/0000-0002-0691-3631; Email: katarzyna.grzybowska@us.edu.pl

Authors

Andrzej Grzybowski − *Institute of Physics, University of Silesia in Katowice, 41-500 Chorzów, Poland; Silesian Center for Education and Interdisciplinary Research, 41-500 Chorzów, Poland;* orcid.org/0000-0002-5258-6926

Justyna Knapik-Kowalczuk − *Institute of Physics, University of Silesia in Katowice, 41-500 Chorzów, Poland; Silesian Center for Education and Interdisciplinary Research, 41-500 Chorzów, Poland;* orcid.org/0000-0003-3736-8098

Krzysztof Chmiel − *Institute of Physics, University of Silesia in Katowice, 41-500 Chorzów, Poland; Silesian Center for Education and Interdisciplinary Research, 41-500 Chorzów, Poland;* orcid.org/0000-0003-4532-0051

Krzysztof Woyna-Orlewicz − *Faculty of Pharmacy, Department of Pharmaceutical Technology and Biopharmaceutics, Jagiellonian University Medical College, 30-688 Kraków, Poland*

Joanna Szafraniec-Szczęsny − *Faculty of Pharmacy, Department of Pharmaceutical Technology and Biopharmaceutics, Jagiellonian University Medical College, 30-688 Kraków, Poland*

Agata Antosik-Rogóż − *Faculty of Pharmacy, Department of Pharmaceutical Technology and Biopharmaceutics, Jagiellonian University Medical College, 30-688 Kraków, Poland*

Renata Jachowicz − *Faculty of Pharmacy, Department of Pharmaceutical Technology and Biopharmaceutics, Jagiellonian University Medical College, 30-688 Kraków, Poland*

Katarzyna Kowalska-Szojda − *Institute of Chemistry, University of Silesia in Katowice, 40-006 Katowice, Poland*

Piotr Lodowski − *Institute of Chemistry, University of Silesia in Katowice, 40-006 Katowice, Poland*

Marian Paluch − *Institute of Physics, University of Silesia in Katowice, 41-500 Chorzów, Poland; Silesian Center for Education and Interdisciplinary Research, 41-500 Chorzów, Poland*

Complete contact information is available at: https://pubs.acs.org/10.1021/acs.molpharmaceut.0c00517

Notes

The authors declare no competing financial interest.

ACKNOWLEDGMENTS

The authors are grateful for the financial support received within the project no. 2015/16/W/NZ7/00404 (SYMFONIA 3) from the National Science Centre, Poland. It should be noted that the Gaussian calculations were carried out in the Wrocław Centre for Networking and Supercomputing, WCSS, Wrocław, Poland, http://www.wcss.wroc.pl, under computational Grant No. 18.

REFERENCES

(1) Amidon, G. L.; Lennernäs, H.; Shah, V. P.; Crison, J. R. A theoretical basis for a biopharmaceutic drug classification: The correlation of *in vitro* drug product dissolution and *in vitro* bioavailability. *Pharm. Res.* **1995**, *12*, 413−420.

(2) Patel, R.; Patel, N.; Patel, N. M. A novel approach for dissolution enhancement of Ibuprofen by preparing floating granules. *Int. J. Res. Pharm. Sci.* **2010**, *1*, 57−64.

(3) Yu, L. Amorphous pharmaceutical solids: preparation, characterization and stabilization. *Adv. Drug Delivery Rev.* **2001**, *48*, 27−42.

(4) Kawakami, K. Current Status of Amorphous Formulation and OtherSpecial Dosage Forms as Formulations for EarlyClinical Phases. *J. Pharm. Sci.* **2009**, *98*, 2875−2885.

(5) Craig, D. Q.; Royall, P. G.; Kett, V. L.; Hopton, M. L. The relevance of the amorphous state to pharmaceutical dosage forms: glassy drugs and freeze dried systems. *Int. J. Pharm.* **1999**, *179*, 179−207.

(6) Murdande, B. S.; Pikal, M. J.; Shanker, R. M.; Bogner, R. H. Solubility Advantage of Amorphous Pharmaceuticals: I. A Thermodynamic Analysis. *Pharm. Res.* **2010**, *27*, 2704−2714.

(7) Murdande, B. S.; Pikal, M. J.; Shanker, R. M.; Bogner, R. H. Solubility Advantage of Amorphous Pharmaceuticals, Part 3: Is Maximum Solubility Advantage Experimentally Attainable and Sustainable? *J. Pharm. Sci.* **2011**, *100*, 4349−4356.

(8) Adrjanowicz, K.; Kaminski, K.; Paluch, M.; Wlodarczyk, P.; Grzybowska, K.; Wojnarowska, Z.; Hawelek, L.; Sawicki, W.; Lepek, P.; Lunio, R. Dielectric relaxation studies and dissolution behavior of amorphous verapamil hydrochloride. *J. Pharm. Sci.* **2010**, *99*, 828−839.
(9) Hancock, B. C.; Parks, M. What is the True Solubility Advantage data for the melting point, heat of fusion, and heat capacity of for Amorphous Pharmaceuticals? *Pharm. Res.* **2000**, *17*, 397−404.
(10) Grzybowska, K.; Paluch, M.; Wlodarczyk, P.; Grzybowski, A.; Kaminski, K.; Hawelek, L.; Zakowiecki, D.; Kasprzycka, A.; Jankowska-Sumara, I. Enhancement of amorphous celecoxib stability by mixing it with octaacetylmaltose: the molecular dynamics study. *Mol. Pharmaceutics* **2012**, *9*, 894−904.
(11) Adrjanowicz, K.; Grzybowska, K.; Kaminski, K.; Hawelek, L.; Paluch, M.; Zakowiecki, D. Comprehensive studies on physical and chemical stability in liquid and glassy states of telmisartan (TEL): solubility advantages given by cryomilled and quenched material. *Philos. Mag.* **2011**, *91*, 1926−1948.
(12) Kaminski, K.; Adrjanowicz, K.; Wojnarowska, Z.; Grzybowska, K.; Hawelek, L.; Paluch, M.; Zakowiecki, D.; Mazgalski, J. Molecular dynamics of the cryomilled base and hydrochloride ziprasidones by means of dielectric spectroscopy. *J. Pharm. Sci.* **2011**, *100*, 2642−2657.
(13) Hancock, B. C.; Zografi, G. Characteristics and significance of the amorphous state in pharmaceutical systems. *J. Pharm. Sci.* **1997**, *86*, 1−12.
(14) Bhugra, C.; Pikal, M. J. Role of thermodynamic, molecular, and kinetic factors in crystallization from the amorphous state. *J. Pharm. Sci.* **2008**, *97*, 1329−1349.
(15) Shamblin, S. L.; Tang, X.; Chang, L.; Hancock, B. C.; Pikal, M. J. Characterization of the time scales of molecular motion in pharmaceutically important glasses. *J. Phys. Chem. B* **1999**, *103*, 4113−4121.
(16) Grzybowska, K.; Capaccioli, S.; Paluch, M. Recent developments in the experimental investigations of relaxations in pharmaceuticals by dielectric techniques at ambient and elevated pressure. *Adv. Drug Delivery Rev.* **2016**, *100*, 158−182.
(17) Teja, S. B.; Patil, S. P.; Shete, G.; Patel, S.; Bansal, A. K. Drug-excipient behavior in polymeric amorphous solid dispersions. *J. Excipients and Food Chem.* **2013**, *4*, 70−94.
(18) Van Drooge, D.; Hinrichs, W.; Frijlink, H. Anomalous dissolution behavior of tablets prepared from sugar glass-based solid dispersions. *J. Controlled Release* **2004**, *97*, 441−452.
(19) Gupta, P.; Bansal, A. K. Spray drying for generation of a ternary amorphous system of celecoxib, PVP, and meglumine. *Pharm. Dev. Technol.* **2005**, *10*, 273−281.
(20) Grzybowska, K.; Chmiel, K.; Knapik, J.; Grzybowski, A.; Jurkiewicz, K.; Paluch, M. Molecular factors governing the liquid and glassy states recrystallization of celecoxib in binary mixtures with excipients of different molecular weights. *Mol. Pharmaceutics* **2017**, *14*, 1154−1168.
(21) Kaminska, E.; Tarnacka, M.; Wlodarczyk, P.; Jurkiewicz, K.; Kolodziejczyk, K.; Dulski, M.; Haznar-Garbacz, D.; Hawelek, L.; Kaminski, K.; Wlodarczyk, A.; Paluch, M. Studying the Impact of Modified Saccharides on the Molecular Dynamics and Crystallization Tendencies of Model API Nifedipine. *Mol. Pharmaceutics* **2015**, *12*, 3007−3019.
(22) Kaminska, E.; Adrjanowicz, K.; Zakowiecki, D.; Milanowski, B.; Tarnacka, M.; Hawelek, L.; Dulski, M.; Pilch, J.; Smolka, W.; Kaczmarczyk-Sedlak, I.; Kaminski, K. Enhancement of the physical stability of amorphous indomethacin by mixing it with octaacetylmaltose. inter and intra molecular studies. *Pharm. Res.* **2014**, *31*, 2887−903.
(23) Goldberg, A. H.; Gibaldi, M.; Kanig, J. L.; Mayersohn, M. Increasing Dissolution Rates and Gastrointestinal Absorption of Drugs Via Solid Solutions and Eutectic Mixtures IV. *J. Pharm. Sci.* **1966**, *55*, 581−583.
(24) Löbmann, K.; Grohganz, H.; Laitinen, R.; Strachan, C.; Rades, T. Amino acids as co-amorphous stabilisers for poorly water soluble drugs-Part 1: Preparation, stability and dissolution enhancement. *Eur. J. Pharm. Biopharm.* **2013**, *85*, 873−881.
(25) Goldberg, A. H.; Gibaldi, M.; Kanig, J. L. Increasing dissolution rates and gastrointestinal absorption of drugs via solid solutions and eutectic mixtures III: Experimental evaluation of griseofulvin-succinic acid solid solution. *J. Pharm. Sci.* **1966**, *55*, 487−492.
(26) Vaka, S. R. K.; Bommana, M. M.; Desai, D.; Djordjevic, J.; Phuapradit, W.; Shah, N. Excipients for amorphous solid dispersions, Amorphous solid Dispersions. In *Amorphous Solid Dispersions*; Shah, N., Sandhu, H., Choi, D. S., Chokshi, H., Malick, A. W., Eds.; Springer: New York, NY, USA, 2014; pp 123−161.
(27) Karagianni, A.; Kachrimanis, K.; Nikolakakis, I. Co-Amorphous Solid Dispersions for Solubility and Absorption Improvement of Drugs: Composition, Preparation, Characterization and Formulations for Oral Delivery. *Pharmaceutics* **2018**, *10*, 98.
(28) Dengale, S. J.; Grohganz, H.; Rades, T.; Löbmann, K. Recent advances in co-amorphous drug formulations. *Adv. Drug Delivery Rev.* **2016**, *100*, 116−125.
(29) Teja, S. B.; Patil, S. P.; Shete, G.; Patel, S.; Bansal, A. K. Drug-excipient behavior in polymeric amorphous solid dispersions. *J. Excipients and Food Chem.* **2013**, *4*, 70−94.
(30) Kothari, K.; Ragoonanan, V.; Suryanarayanan, R. The Role of Drug - Polymer Hydrogen Bonding Interactions on the Molecular Mobility and Physical Stability of Nifedipine Solid Dispersions. *Mol. Pharmaceutics* **2015**, *12*, 162−170.
(31) Meng, F.; Trivino, A.; Prasad, D.; Chauhan, H. Investigation and correlation of drug polymer miscibility and molecular interactions by various approaches for the preparation of amorphous solid dispersions. *Eur. J. Pharm. Sci.* **2015**, *71*, 12−24.
(32) Taylor, L. S.; Zografi, G. Spectroscopic characterization of interactions between PVP and indomethacin in amorphous molecular dispersions. *Pharm. Res.* **1997**, *14*, 1691−1698.
(33) Kothari, K.; Ragoonanan, V.; Suryanarayanan, R. The Role of Drug - Polymer Hydrogen Bonding Interactions on the Molecular Mobility and Physical Stability of Nifedipine Solid Dispersions. *Mol. Pharmaceutics* **2015**, *12*, 162−170.
(34) Kaminska, E.; Adrjanowicz, K.; Kaminski, K.; Wlodarczyk, P.; Hawelek, L.; Kolodziejczyk, K.; Tarnacka, M.; Zakowiecki, D.; Kaczmarczyk-Sedlak, I.; Pilch, J.; Paluch, M. A new way of stabilization of furosemide upon cryogenic grinding by using acylated saccharides matrices. The role of hydrogen bonds in decomposition mechanism. *Mol. Pharmaceutics* **2013**, *10*, 1824−1835.
(35) Becke, A. D. The role of exact exchange. *J. Chem. Phys.* **1993**, *98*, 5648−5652.
(36) Becke, A. D. Density-functional exchange-energy approximation with correct asymptotic behaviour. *Phys. Rev. A: At., Mol., Opt. Phys.* **1988**, *38*, 3098−3100.
(37) Lee, C.; Yang, W.; Parr, R. G. Development of the Colle-Salvetti correlation-energy formula into a functional of the electron density. *Phys. Rev. B: Condens. Matter Mater. Phys.* **1988**, *37*, 785−789.
(38) Weigend, F.; Ahlrichs, R. Balanced basis sets of split valence, triple zeta valence and quadruple zeta valence quality for H to Rn: Design and assessment of accuracy. *Phys. Chem. Chem. Phys.* **2005**, *7*, 3297−305.
(39) Scalmani, G.; Frisch, M. J. Continuous surface charge polarizable continuum models of solvation. I. general formalism. *J. Chem. Phys.* **2010**, *132*, 114110.
(40) Tomasi, J.; Mennucci, B.; Cammi, R. Quantum mechanical continuum solvation models. *Chem. Rev.* **2005**, *105*, 2999−3093.
(41) Grimme, S.; Antony, J.; Ehrlich, S.; Krieg, H. A consistent and accurate ab initio parameterization of density functional dispersion correction (DFT-D) for the 94 elements H-Pu. *J. Chem. Phys.* **2010**, *132*, 154104.
(42) Frisch, M. J.; Trucks, G. W.; Schlegel, H. B.; Scuseria, G. E.; Robb, M. A.; Cheeseman, J. R.; Scalmani, G.; Barone, V.; Petersson, G. A.; Nakatsuji, H.; Li, X.; Caricato, M.; Marenich, A.; Bloino, J.; Janesko, B. G.; Gomperts, R.; Mennucci, B.; Hratchian, H. P.; Ortiz, J. V.; Izmaylov, A. F.; Sonnenberg, J. L.; Williams-Young, D.; Ding, F.; Lipparini, F.; Egidi, F.; Goings, J.; Peng, B.; Petrone, A.; Henderson,

https://dx.doi.org/10.1021/acs.molpharmaceut.0c00517
Mol. Pharmaceutics 2020, 17, 3087−3105

T.; Ranasinghe, D.; Zakrzewski, V. G.; Gao, J.; Rega, N.; Zheng, G.; Liang, W.; Hada, M.; Ehara, M.; Toyota, K.; Fukuda, R.; Hasegawa, J.; Ishida, M.; Nakajima, T.; Honda, Y.; Kitao, O.; Nakai, H.; Vreven, T.; Throssell, K.; Montgomery, Jr., J. A.; Peralta, J. E.; Ogliaro, F.; Bearpark, M.; Heyd, J. J.; Brothers, E.; Kudin, K. N.; Staroverov, V. N.; Keith, T.; Kobayashi, R.; Normand, J.; Raghavachari, K.; Rendell, A.; Burant, J. C.; Iyengar, S. S.; Tomasi, J.; Cossi, M.; Millam, J. M.; Klene, M.; Adamo, C.; Cammi, R.; Ochterski, J. W.; Martin, R. L.; Morokuma, K.; Farkas, O.; Foresman, J. B.; Fox, D. J. *Gaussian 09*, Revision E.01; Wallingford, CT, 2016.

(43) Power, G.; Vij, J. K.; Johari, G. P. Relaxations and nano-phase-separation in ultraviscous heptanol-alkyl halide mixture. *J. Chem. Phys.* **2007**, *126*, 034512.

(44) Grzybowska, K.; Grzybowski, A.; Pawlus, S.; Hensel-Bielowka, S.; Paluch, M. Dielectric relaxation processes in water mixtures of tripropylene glycol. *J. Chem. Phys.* **2005**, *123*, 204506.

(45) Grzybowska, K.; Paluch, M.; Grzybowski, A.; Pawlus, S.; Ancherbak, S.; Prevosto, D.; Capaccioli, S. Dynamic Crossover of Water Relaxation in Aqueous Mixtures: Effect of Pressure. *J. Phys. Chem. Lett.* **2010**, *1*, 1170−1175.

(46) Harmandaris, V. A.; Kremer, K.; Floudas, G. Dynamic Heterogeneity in Fully Miscible Blends of Polystyrene with Oligostyrene. *Phys. Rev. Lett.* **2013**, *110*, 165701.

(47) Brás, A. R.; Noronha, J. P.; Antunes, A. M. M.; Cardoso, M. M.; Schönhals, A.; Affouard, F.; Dionísio, M.; Correia, N. T. Molecular Motions in Amorphous Ibuprofen As Studied by Broadband Dielectric Spectroscopy. *J. Phys. Chem. B* **2008**, *112*, 11087−11099.

(48) Adrjanowicz, K.; Kaminski, K.; Wojnarowska, Z.; Dulski, M.; Hawelek, L.; Pawlus, S.; Paluch, M.; Sawicki, W. Dielectric Relaxation and Crystallization Kinetics of Ibuprofen at Ambient and Elevated Pressure. *J. Phys. Chem. B* **2010**, *114*, 6579−6593.

(49) Ottou Abe, M. T.; Correia, N. T.; Ndjaka, J. M. B.; Affouard, F. A comparative study of ibuprofen and ketoprofen glass-forming liquids by molecular dynamics simulations. *J. Chem. Phys.* **2015**, *143*, 164506.

(50) Affouard, F.; Correia, N. T. Debye Process in Ibuprofen Glass-Forming Liquid: Insights from Molecular Dynamics Simulation. *J. Phys. Chem. B* **2010**, *114*, 11397−11402.

(51) Adrjanowicz, K.; Kaminski, K.; Dulski, M.; Wlodarczyk, P.; Bartkowiak, G.; Popenda, L.; Jurga, S.; Kujawski, J.; Kruk, J.; Bernard, M. K.; Paluch, M. Communication: Synperiplanar to antiperiplanar conformation changes as underlying the mechanism of Debye process in supercooled ibuprofen. *J. Chem. Phys.* **2013**, *139*, 111103.

(52) Zhou, D.; Zhang, G. G. Z.; Law, D.; Grant, D. J. W.; Schmitt, E. A. Physical stability of amorphous pharmaceuticals: Importance of configurational thermodynamic quantities and molecular mobility. *J. Pharm. Sci.* **2002**, *91*, 1863−1872.

(53) Bhugra, C.; Telang, C.; Schwabe, R.; Zhong, L. Reduced Crystallization Temperature Methodology for Polymer Selection in Amorphous Solid Dispersions: Stability Perspective. *Mol. Pharmaceutics* **2016**, *13*, 3326−3333.

(54) Havriliak, S.; Negami, S. A complex plane analysis of a-dispersions in some polymer systems. *J. Polym. Sci., Part C: Polym. Symp.* **1966**, *14*, 99−117.

(55) Havriliak, S.; Negami, S. A complex plane representation of dielectric and mechanical relaxation processes in some polymers. *Polymer* **1967**, *8*, 161−210.

(56) Vogel, H. Das Temperaturabhangigkeitgesetz der Viskosität von Flüssigkeiten. *J. Phys. Z.* **1921**, *22*, 645−646.

(57) Fulcher, G. S. Analysis of Recent Measurements of the Viscosity of Glasses. *J. Am. Ceram. Soc.* **1925**, *8*, 339−355.

(58) Tammann, G.; Hesse, W. Die Abhängigkeit der Viscosität von der Temperatur bie unterkühlten Flüssigkeiten. *Z. Anorg. Allg. Chem.* **1926**, *156*, 245−257.

(59) Couchman, P. R.; Karasz, F. E. A classical thermodynamic discussion on the effect of composition on glass-transition temperatures. *Macromolecules* **1978**, *11*, 117−119.

(60) Shamblin, S.; Taylor, L.; Zografi, G. Mixing Behavior of Colyophilized Binary Systems. *J. Pharm. Sci.* **1998**, *87*, 694−701.

(61) Williams, G. Complex dielectric constant of dipolar compounds as a function of temperature, pressure and frequency. Part 1. General relations and a consideration of models for relaxation. *Trans. Faraday Soc.* **1964**, *60*, 1548−1555.

(62) Baird, J. A.; Taylor, L. S. Evaluation of amorphous solid dispersion properties using thermal analysis techniques. *Adv. Drug Delivery Rev.* **2012**, *64*, 396−421.

(63) Baird, J. A.; van Eerdenbrugh, B.; Taylor, L. S. A Classification System to Assess the Crystallization Tendency of Organic Molecules from Undercooled Melts. *J. Pharm. Sci.* **2010**, *99*, 3787−3806.

(64) Rams-Baron, M.; Wojnarowska, Z.; Grzybowska, K.; Dulski, M.; Knapik, J.; Jurkiewicz, K.; Smolka, W.; Sawicki, W.; Ratuszna, A.; Paluch, M. Towards a better understanding of the physical stability of amorphous anti-inflammatory agents: the role of molecular mobility and molecular interaction patterns. *Mol. Pharmaceutics* **2015**, *12*, 3628−3638.

(65) Adam, G.; Gibbs, J. H. On the Temperature Dependence of Cooperative Relaxation Properties in Glass-Forming Liquids. *J. Chem. Phys.* **1965**, *43*, 139−146.

(66) Saiter, A.; Delbreilh, L.; Couderc, H.; Arabeche, K.; Schönhals, A.; Saiter, J.-M. Temperature dependence of the characteristic length scale for glassy dynamics: Combination of dielectric and specific heat spectroscopy. *Phys. Rev. E* **2010**, *81*, 041805.

(67) Berthier, L.; Biroli, G.; Bouchaud, J.-P.; Jack, R. L. Overview of different characterizations of dynamic heterogeneity. In *Dynamical Heterogeneities in Glasses, Colloids, and Granular Media*; Berthier, L., Biroli, G., Bouchaud, J.-P., Cipelletti, L., van Saarloos, W., Eds.; Oxford University Press, 2011; Chapter 3.

(68) Donth, E. The size of cooperatively rearranging regions at the glass transition. *J. Non-Cryst. Solids* **1982**, *53*, 325−330.

(69) Donth, E. *The Glass Transition, Relaxation Dynamics in Liquids and Disordered Materials*; Springer: Berlin, 2001.

(70) Berthier, L.; Biroli, G.; Bouchaud, J.-P.; Cipelletti, L.; El Masri, D.; L'Hôte, D.; Ladieu, F.; Pierno, M. Direct Experimental Evidence of a Growing Length Scale Accompanying the Glass Transition. *Science* **2005**, *310*, 1797−1800.

(71) Hempel, E.; Hempel, G.; Hensel, A.; Schick, C.; Donth, E. Characteristic length of dynamic glass transition near T_g for a wide assortment of glass-forming substances. *J. Phys. Chem. B* **2000**, *104*, 2460−2466.

(72) Dalle-Ferrier, C.; Thibierge, C.; Alba-Simionesco, C.; Berthier, L.; Biroli, G.; Bouchaud, J.-P.; Ladieu, F.; L'Hôte, D.; Tarjus, G. Spatial correlations in the dynamics of glassforming liquids: Experimental determination of their temperature dependence. *Phys. Rev. E* **2007**, *76*, 041510.

(73) Grzybowska, K.; Grzybowski, A.; Wojnarowska, Z.; Knapik, J.; Paluch, M. Ionic liquids and their bases: Striking differences in the dynamic heterogeneity near the glass transition. *Sci. Rep.* **2015**, *5*, 16876.

(74) Shintani, H.; Tanaka, H. Frustration on the way to crystallization in glass. *Nat. Phys.* **2006**, *2*, 200−206.

(75) Kawasaki, T.; Araki, T.; Tanaka, H. Correlation between Dynamic Heterogeneity and Medium-Range Order in Two-Dimensional Glass-Forming Liquids. *Phys. Rev. Lett.* **2007**, *99*, 215701.

(76) Tah, I.; Sengupta, S.; Sastry, S.; Dasgupta, C.; Karmakar, S. Glass Transition in Supercooled Liquids with Medium-Range Crystalline Order. *Phys. Rev. Lett.* **2018**, *121*, 085703.

(77) Kawakami, K. Dynamics of ribavirin glass in the sub-Tg temperature region. *J. Phys. Chem. B* **2011**, *115*, 11375−11381.

(78) Kolodziejczyk, K.; Paluch, M.; Grzybowska, K.; Grzybowski, A.; Wojnarowska, Z.; Hawelek, L.; Ziolo, J. D. Relaxation dynamics and crystallization study of sildenafil in the liquid and glassy states. *Mol. Pharmaceutics* **2013**, *10*, 2270−2282.

(79) Bhattacharya, S.; Suryanarayanan, R. Local mobility in amorphous pharmaceuticals—characterization and implications on stability. *J. Pharm. Sci.* **2009**, *98*, 2935−2953.

(80) Kissi, E. O.; Grohganz, H.; Löbmann, K.; Ruggiero, M. T.; Zeitler, J. A.; Rades, T. Glass-Transition Temperature of the *β*-

https://dx.doi.org/10.1021/acs.molpharmaceut.0c00517
Mol. Pharmaceutics 2020, 17, 3087−3105

Relaxation as the Major Predictive Parameter for Recrystallization of Neat Amorphous Drugs. *J. Phys. Chem. B* **2018**, *122*, 2803−2808.
(81) Ngai, K. L.; Paluch, M. Classification of secondary relaxation in glass-formers based on dynamic properties. *J. Chem. Phys.* **2004**, *120*, 857−873.

https://dx.doi.org/10.1021/acs.molpharmaceut.0c00517
Mol. Pharmaceutics 2020, 17, 3087−3105